Manuscript for *Hydrology and Earth System Science*   March 26, 2024

Elevational Control of Isotopic Composition and Application in Understanding Hydrologic Processes in the mid Merced River Catchment, Sierra Nevada, California, USA

Fengjing Liu[1, a], Martha H. Conklin[2], and Glenn D. Shaw [3]

[1] College of Forest Resources and Environmental Science,

Michigan Technological University, Houghton, MI 49931, USA

[2] Sierra Nevada Research Institute & School of Engineering,

University of California, Merced, CA95343, USA

[3] Department of Geological Engineering, Montana Tech of the University of Montana, Butte, MT59701, USA

ª Corresponding Address†

Fengjing Liu

College of Forest Resources and Environmental Science

Michigan Technological University

1400 Townsend Drive

Houghton, MI 49931

Phone: 906-487-1089

Email: fliu7@mtu.edu

30   **Abstract.** Mountain snowpack has been declining and more precipitation has fallen as rainfall than snowfall, particularly in the US West. Isotopic composition in stream water, springs, groundwater, and precipitation was examined to understand the impact of declining snowpack on hydrologic processes in the mid Merced River catchment (1,873 km^2), Sierra Nevada, California. Mean isotopic values in small tributaries (catchment area<122 km^2), rock glacier outflows and

35   groundwater from 2005-2008 were strongly correlated with mean catchment elevation (R^2 = 0.96 for δ^{2}H, *n*=16, *p*<0.001), with an average isotopic lapse rate of -1.9‰/100 m for δ^{2}H and -0.22‰/100 m for δ^{18}O in meteoric water. The lapse rate did not change much over seasons and was not strongly affected by isotopic fractionation. A catchment-characteristic isotopic value, representing catchment arithmetic mean isotopic signature in meteoric water, was thus established

40   for each sub-catchment based on the lapse rate to elucidate hydrometeorologic and hydrologic processes such as the duration and the magnitude of snowmelt events and elevational water sources of stream flow and groundwater for ungagged catchments. Compared to Tenaya Creek without water falls, flow and flow duration of Yosemite Creek appear to be much more sensitive to seasonal temperature increase during the baseflow period due to a strong evaporation effect caused

45   by waterfalls, suggesting possible prolonged dry-up period of Yosemite Falls in the future. Groundwater in the Yosemite Valley (~900-1,200 m) was recharged primarily from the upper snow-rain transition zone (2,000-2,500 m), suggesting its strong vulnerability to shift in snow-rain ratio. The information gained from this study helps advance our understanding of hydrologic responses to climate change in snowmelt-fed river systems.

50

    Key Words: Stable isotopes, isotopic lapse rate, groundwater recharge, snow-rain transition, Yosemite Falls, Merced River

55

60

1. Introduction

With an increase in global temperature, snow cover extent has decreased in the Northern Hemisphere, especially in spring (*Vaughan et al*., 2013). In the mountain regions of the U.S. West, less precipitation falls as snow (e.g., *Mote et al*., 2005; *Knowles et al*., 2006) and the melting of snow starts earlier (e.g., *Stewart et al*., 2004). Even without any changes in precipitation amount, observations and modeling results have shown that less snow and earlier snowmelt lead to a shift in peak river runoff toward late winter and early spring, away from summer when water demand is highest (e.g., *Dettinger and Cayan*, 1995; *Barnett et al*., 2005; *Stewart et al*., 2005). A decrease in snow to rain ratio also reduces groundwater recharge within the mountain block (*Earman* et al., 2006; 2011; *Penna et al*., 2014). It is anticipated that these changes in snow condition and subsequent responses of stream flow and groundwater recharge are strongest in the snow-rain transition zone (e.g., *Tennant et al*., 2015), which is 1,500-2,500 m in Sierra Nevada, California based on *Hunsaker et al*. (2012).

However, our present knowledge of watershed hydrology is still not sufficient to fully understand the impact of these changes on stream flow and groundwater recharge (*Kundzewicz et al*., 2007; *Alley*, 2001; *Fayad et al*., 2017). Particularly for catchments with a Mediterranean climate such as those in Sierra Nevada, California and Europe, where precipitation is little after the snowmelt season in spring and early summer, it is unclear how the changes in snow condition in spring affects baseflow (stream flow after snowmelt period or low flow) in late summer and fall (*Fayad et al*., 2017). This problem is primarily caused by lack of accurate hydrologic measurements in mountains (*Bales et al*., 2006) and adequate techniques to determine groundwater recharge generated from snowmelt and rainwater (*Wilson and Guan*, 2004; *Manning & Solomon*, 2005; *Manning & Caine*, 2007).

Stable isotopes of oxygen and hydrogen in the water molecule have become an important tool for studies on atmospheric processes (e.g., *Gat*, 1996; *Friedman et al.*, 2002; *Peng et al*., 2016; *Balagizi et al*., 2018), palaeoclimate (e.g., *Thompson et al*., 2000), and watershed hydrology (*e.g*., *Araguas-Araguas et al*., 2000). In watershed hydrology, the isotopic composition has been widely applied to study the origin and dynamics of stream water and groundwater across varying climates and land covers from snow-dominated catchments in high elevations to forested catchments in temperate regions (*e.g*., *Kendall and McDonnell*, 1998; *Wen et al.*, 2016; *Penna et al.*, 2017). The distinctness of isotopic composition among source waters (endmembers) is the basis for the studies

of watershed hydrology and allows identification and even quantification of the contributions of source waters to stream flow (e.g., *Sklash et al.*, 1976; *Liu et al.*, 2004; *Penna et al.*, 2016). It is also well-known that elevation exerts a strong control on isotopic composition in meteoric water (e.g., *Jodar et al.*, 2016; *Peng et al.*, 2016), stream water (e.g., *Jeelani et al.*, 2013; *Voss et al.*, 2020), and groundwater (e.g., *Ingraham and Taylor*, 1991). The isotopic lapse rate, change in isotopic composition over elevations (usually in δ/100m), was used to reconstruct paleoelevations (e.g., *Poage and Chamberlain*, 2001) and determine groundwater recharge zones (e.g., O'*Driscoll et al.*, 2005; *Jeelani et al.*, 2010; *Koeniger et al.*, 2017). However, the isotopic lapse rate in meteoric water and stream water may be complicated by isotopic fractionation during snow formation and snowmelt processes (e.g., *Taylor et al.*, 2001), seasonal variation in climate (e.g., *Voss et al.*, 2020), and evaporation processes and sublimation of snow (e.g., *Peng et al.*, 2015). The success of the applications using stable isotopes hinges on our understanding of the processes or factors that control the isotopic composition in the studied subject (e.g., stream water, groundwater, water vapor, and snow).

As the first step in an ongoing effort to quantify how change in the snow-rain proportion affects stream flow and groundwater recharge in a snowmelt-fed river system, the objectives of this study were to understand the processes or factors that control the spatiotemporal variation of isotopic composition in precipitation, stream water and groundwater and how such information could be used to advance our understanding of hydrometeorologic and hydrologic processes in a snowmelt-fed river system. Specifically, we examined (1) how well elevation controls isotopic composition in snow, stream water, and groundwater; (2) how to establish a lapse rate of isotopic composition in meteoric water (e.g., using precipitation samples or stream samples); (3) how the lapse rate varies with season and isotopic fractionation; and (4) how one can best use the lapse rate in understanding the impact of the shifts in snow-rain on groundwater recharge and other hydrologic processes. This study was conducted in the Merced River above Briceburg (mid Merced River catchment) (Figure 1), a representative snowmelt-fed river system for the central and southern Sierra Nevada, California. Isotopic data were acquired from precipitation, springs, groundwater, and stream water during the 2005-2008 period, which includes a very wet year (2006) and a very dry year (2007). The data from such a period thus provides us with an excellent opportunity to examine the variability of stable isotopic composition in surface water and groundwater with precipitation extremes in the mid Merced River catchment.
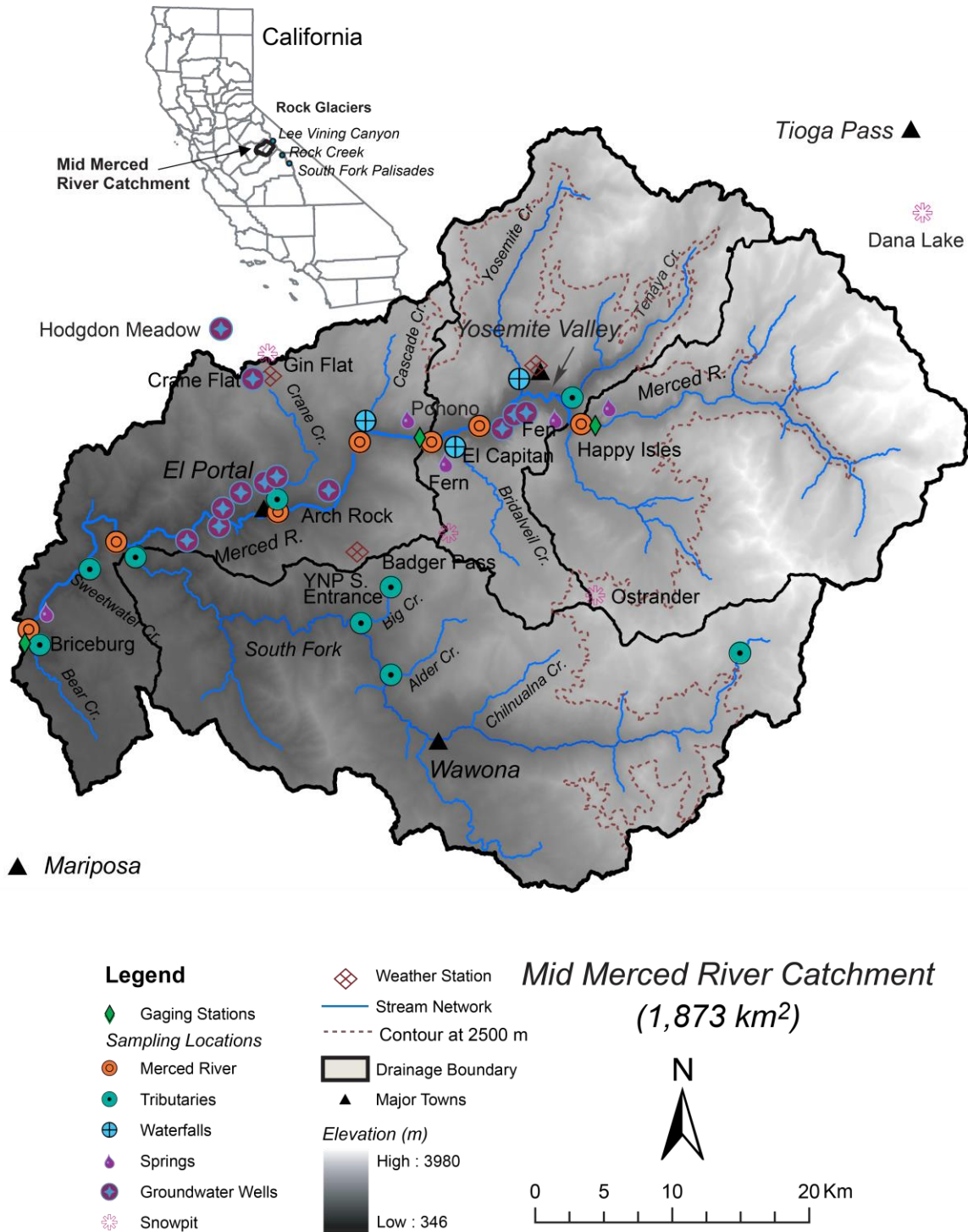
Figure 1. Sampling locations for snow, stream water, spring water and groundwater in the mid Merced River catchment, along with stream gages and meteorological stations, topography, stream network and drainage boundary. The inset map shows the locations of the mid Merced River catchment in California and rock glaciers outside the catchment. The elevation contour at 2,500 m (brown dashed line) is also marked to show the upper boundary of the snow-rain transition zone.

2. Research site

130   The study was conducted in the mid Merced River catchment above Briceburg, including Yosemite Valley (Figure 1). The mid Merced River catchment drains 1,873 km^2, and ranges in elevation from 346 m at Briceburg to 3,993 m eastward at the crest. The drainage is relatively undisturbed by human activities such as dams, much of it within Yosemite National Park (YNP). The mid Merced River was designated a Wild and Scenic River in 1987 by the U.S. Congress.

135   The mid Merced River catchment is characterized by a Mediterranean climate, with moderately wet, cold winters and dry, warmer summers. The mean annual precipitation at the Yosemite Valley (Figure 1) has been 916 mm, based on data from 1917 to 2008. Precipitation in the region occurs primarily from October to April, mainly as snow above 2,500 m and rain below 1,500 m, as shown by meteorological data at a neighboring site in the southern Sierra Nevada,

140   about 100 miles south to the Merced River (*Hunsaker et al*., 2012). Precipitation from May to October accounted for only 25% of the annual mean precipitation. Air temperature gradually decreased with elevation, with a lapse rate of approximately 1°C/100m, while snow water equivalent (SWE) increased with elevation (Rice et al., 2011). Combining with measured SWE and remotely sensed snow covers, *Rice et al*. (2011) estimated that SWE increased by 11.0

145   cm/100m with elevation in 2004 and 2005.

        Like most of the Sierra Nevada range, the mid Merced River catchment is underlain by granitic rocks of the Sierra Nevada batholith. Most of the rocks are part of the Tuolumne Intrusive Suite, a group of four concentrically arranged plutonic bodies, within which are all granites and granodiorites (*Bateman*, 1992). Vegetation covers approximately 45% of the catchment and

150   includes a red fir forest that grades into a mixed subalpine forest above 2,750 m (*Rundel et al*., 1977). Above the timberline (~3,200 m), the vegetation consists of low-lying tundra plants and alpine meadow vegetation. Surficial deposits cover about 20% of the catchment above Happy Isles and valleys are covered primarily by glacial tills that occur in valley bottoms as lateral and recessional moraines (*Clow et al*., 1996). Wells drilled in the Yosemite Valley indicate that the

155   deposit is about 300 m, consistent with *Gutenburg et al.* (1956), which is dominated by unconsolidated sands from land surface to about 20 m below, mainly silt from 20 m to 70 m, granitic gravels in silt from 70 m to 80 m, and chiefly boulders and sands below 80 m. The deposit in the lower section of the catchment from El Portal to Briceburg is approximately 20 m in depth, consisting of gravels, cobbles, decomposed granite, sand and silt.

3. Methods

3.1. Hydrologic and meteorological data

Hydrologic and meteorological data were downloaded from the California Data Exchange Center (CDEC; https://cdec.water.ca.gov; access verified on August 17, 2023). Stream flow was measured at Happy Isles and Pohono Bridge (data also available for both sites at https://waterdata.usgs.gov/usa/nwis; access verified on August 17, 2023) (Figure 1) by the United States Geological Survey (USGS) and daily mean discharges were used in the study. Happy Isles is a USGS Hydrologic Benchmark Network site; this network was developed, in part, for its utility as a long-term monitoring network designed for detection of trends in stream flow and chemistry in response to changes in climate (*Mast and Clow*, 2000). Note that stream flow at Briceburg was measured by the Merced Irrigation District. The stage sensor at Briceburg is located inside of a stilling well from which water is pumped out to supply water for the city of Mariposa, which may cause water level to drop several feet during short periods. The stream flow data at Briceburg was thus used with care in this study. Precipitation was measured at Yosemite Valley, Gin Flat and Wawona by the Yosemite National Park and the California Department of Water Resources. Snow depth was measured by snow courses, operated by the California Department of Water Resources and U.S. Natural Resource Conservation Service, and the daily values at Gin Flat, Ostrander and Tioga Pass were selected. Daily snow water equivalent (SWE) data was not available for all stations and thus snow depth was used in this study. Snow depth data from other stations in the catchment was not selected because daily values were not available. Tioga Pass, located just outside the catchment, was selected because it is the only one located above 3,000 m in the region.

3.2. Sample collection

Samples of stream water, groundwater, and spring water were collected from the 2005-2008 period through extensive field campaigns in the mid Merced River catchment (Figure 1 and Table 1). Stream water samples were collected weekly to biweekly at about twenty locations along the Merced River, including gages at Happy Isles, Pohono Bridge and Briceburg, and major tributaries. Note that samples of Merced River at Cascade Picnic Area were collected from a spot right after the confluence of Cascade Creek (Figure 1). The Merced River channel is wide-open in that section and the sampling spot is on the same side as Cascade Creek. Water from Merced River and Cascade Creek may not be well mixed at the sampling spot due to the short distance to the

confluence, but a well-mixed spot cannot be established due to local landscape, safety and logistic issues. In addition, an earlier study showed that this area is a groundwater discharge zone (*Shaw et al*., 2014). So, data from this site was used and interpreted cautiously.

195 Table 1. Mean $\delta^{18}O$ and $\delta^{2}H$ values with $\pm1\sigma$ (one standard deviation) in streams, glacier outflows, spring water, groundwater, and precipitation in the mid Merced River catchment and vicinity, along with catchment characteristics.

Type	Locations	Sample Start Date	Sample End Date	Number n	Elevation (m)	Catchment Area (km²)	Catchment Elevation Mean (m)	Catchment Elevation Max (m)	$\delta^{18}O$ Values Mean (‰)	$\delta^{18}O$ Values ±1σ (‰)	$\delta^{2}H$ Values Mean (‰)	$\delta^{2}H$ Values ±1σ (‰)
Merced River	Happy Isles	11/11/2005	8/7/2008	68	1251	468	2743	3993	-13.8	0.9	-102.4	5.1
	El Capitan	11/11/2005	8/7/2005	49	1206	744	2624	3993	-13.4	0.7	-98.8	4.1
	Pohono Bridge	5/19/2006	8/7/2008	64	1179	833	2580	3993	-13.3	0.7	-98.0	4.3
	Cascade Picnic Area	11/11/2005	7/22/2008	37	1040	902	2539	3993	-12.7	0.7	-91.8	4.4
	El Portal	9/1/2006	7/22/2008	35	605	961	2483	3993	-13.1	0.7	-96.5	4.2
	South Fork Confluence	3/30/2006	7/22/2008	33	424	1087	2350	3993	-12.9	1.0	-93.1	5.3
	Briceburg	11/11/2005	7/22/2008	54	346	1873	2067	3993	-12.4	1.1	-90.5	7.5
Tributaries	Tenaya Creek	11/6/2006	8/7/2008	43	1212	122	2528	3310	-13.1	0.6	-95.9	2.6
	Yosemite Creek	11/11/2005	8/7/2008	50	1249	109	2516	3294	-12.0	1.8	-89.2	8.8
	Bridalveil Creek	11/11/2005	8/7/2008	48	1284	64	2232	2837	-12.1	0.7	-87.2	3.6
	Cascade Creek	11/11/2005	6/6/2008	38	1143	50	2228	2736	-12.0	0.6	-85.0	3.6
	Crane Creek	11/11/2005	7/22/2008	37	602	46	1621	2163	-11.4	0.6	-79.6	2.7
	South Fork	11/11/2005	8/4/2008	40	425	623	1857	3575	-11.9	1.2	-85.6	7.0
	Sweetwater Creek	8/21/2006	7/22/2008	32	375	18	1058	1408	-10.2	0.4	-70.4	1.6
	Bear Creek	9/1/2006	6/13/2008	29	348	58	913	1409	-9.0	0.5	-64.2	2.1
	Alder Creek	7/16/2008	8/5/2008	6	1099	39	1806	2446	-12.0	0.3	-85.0	0.8
	Big Creek at Fish Camp	7/16/2008	8/4/2008	6	1515	44	1946	2649	-12.3	0.4	-86.1	0.9
	Big Creek at South Fork	7/16/2008	8/5/2008	6	1203	80	1798	2649	-11.8	0.4	-83.3	0.7
	Headwater of South Fork	8/4/2008	8/4/2008	1	2754	8	2969	3550	-13.0	N/A	-101.3	N/A
Rock Glaciers	Lee Vining Canyon	7/21/2006	7/21/2006	1	2965	1	3271	3531	-15.3	N/A	-115.5	N/A
	South Fork of Palisade	7/20/2006	10/7/2007	6	3289	2	3624	4067	-15.8	0.6	-117.1	5.1
	Rock Creek	8/18/2006	7/15/2007	4	3568	1	3772	4101	-16.6	0.7	-120.2	4.3
Springs	Happy Isles	4/6/2006	8/7/2008	39	1210				-13.5	0.3	-99.0	2.0
	Fen	8/21/2006	8/7/2008	29	1109				-13.7	0.3	-98.3	1.3
	Fern	11/11/2005	8/7/2008	55	1199				-12.3	0.4	-86.8	1.3
	Drinking Fountain	4/6/2006	7/22/2008	25	372				-9.6	0.3	-67.6	1.1
Groundwater	Valley Well 1	6/21/2005	7/15/2008	5	1188				-12.8	0.2	-94.1	1.5
	Valley Well 2	6/21/2005	7/15/2008	5	1180				-12.5	0.2	-91.9	1.1
	Valley Well 4	6/21/2005	7/15/2008	5	1183				-12.7	0.2	-93.5	1.0
	Arch Rock	6/21/2005	10/24/2007	4	933				-12.4	0.1	-89.5	1.2
	Crane Flat	6/21/2005	7/15/2008	5	1994	0.2	2011	2027	-12.4	0.1	-85.9	0.7
	Hodgdon Meadow	6/21/2005	7/15/2008	5	1407	4	1542	1836	-11.5	0.2	-81.5	0.7
	El Portal Well 2	6/21/2005	7/15/2008	5	565				-10.9	0.3	-80.4	2.3
	El Portal Well 3	6/21/2005	7/15/2008	5	571				-11.0	0.4	-81.2	4.3
	El Portal Well 4	6/21/2005	7/15/2008	5	561				-11.9	0.6	-87.2	6.0
	El Portal Well 5	6/21/2005	7/15/2008	5	544				-11.5	0.5	-83.9	3.9
	El Portal Well 6	6/21/2005	7/15/2008	5	567				-12.4	0.3	-90.9	2.1
	El Portal Well 7	6/21/2005	7/15/2008	5	563				-12.6	0.5	-92.7	2.9
Snowpits	Gin Flat	4/27/2006	4/27/2006	23	2150				-11.4	2.0	-82.4	15.6
	Badger Pass	3/27/2006	3/31/2006	13	2226				-13.2	1.2	-93.9	10.5
	Ostrander	3/29/2006	3/29/2006	25	2500				-14.6	2.5	-106.5	21.0
	Dana Lake	8/18/2005	8/18/2005	3	2926				-14.7	1.5	-105.5	12.1
Precipitation	NADP	11/14/2006	4/24/2007	10	1393				-11.5	2.5	-80.2	17.8

200  Water samples were collected from four springs located near the Merced River between Happy Isles and Briceburg (Figure 1), with a frequency varying from weekly to monthly. Water samples were also collected bi-annually during snowmelt and off-snowmelt seasons from 2005 to 2008 from drinking water wells located in Yosemite Valley, El Portal, Crane Flat and Hodgdon Meadow (Figure 1). The depths of wells range from 100 to 120 m in Yosemite Valley and from

205  20 to 30 m at El Portal. Information on the depth of other wells was not available. Samples were taken directly from the sampling ports.

  Water samples were also collected at the outflows of three rock glaciers at the South Fork of Palisade River, Rock Creek and Lee Vining Canyon, just outside the mid Merced River catchment (Figure 1). These samples were collected 1-4 times from July 2006 to October 2007.

210  Snow and rain samples were collected at the National Atmospheric Deposition Program (NADP) site (Site ID = CA99, elevation = 1,393 m) in Yosemite National Park from November 2006 through April 2007. These samples were collected from a rain gage right after storms and only from relatively large storms when there was enough water left over after the NADP samples were collected. These samples were from snowfall, rainfall, and a mixture of snowfall and rainfall

215  based on the collector's notes.

  Three snowpits were excavated near the maximum snow accumulation in late March and early April 2006 at Badger Pass, Gin Flat and Ostrander near Yosemite Valley (Figure 1; Table 1). The depth of snowpits ranges from 1.5 to 2.5 m. Snow samples were collected continuously every 10-cm throughout the entire pit at Badger Pass, Ostrander and Gin Flat. Three snow core

220  samples were collected in summer 2005 at Dana Lake, just below the crest on the eastern side of Sierra Nevada and outside the mid Merced River catchment. Snow samples were stored in plastic bags pre-rinsed with deionized water (DI) and washed by sampling snow at the time of collection. Snow samples were melted at room temperature immediately upon arrival at the laboratory.

  All liquid water samples were stored in 30-mL glass vials with snap-on caps. All samples

225  were checked for the absence of air bubbles. After collection, samples were transported to the University of California, Merced and kept refrigerated at 4 °C until analysis.

3.3. Sample analysis

  The stable isotope ratios ($^{18}O/^{16}O$ and $^2H/^1H$) of all samples are expressed as δ (per mil,

230  expressed as ‰) variation in the ratio of the sample relative to Vienna Standard Mean Ocean Water

(VSMOW). Samples collected in 2005 and 2006 were analyzed at the University of California, Berkeley, using a VG PRISM isotope ratio mass spectrometer, with a precision of 0.05‰ for $\delta^{18}O$ and 0.3‰ for δ^2H. Samples collected in 2007 and 2008 were analyzed using a Los Gatos LTD100 Isotopic Analyzer at the University of California, Merced. This analyzer is based on continuous laser absorption spectroscopy (LAS). The precision of this instrument was comparable to conventional mass spectrometer (*Wang et al*., 2009a), with our data showing 1σ (standard deviation) precision better than 0.2‰ for $\delta^{18}O$ and 0.3‰ for δ^2H, consistent with *Berman et al*. (2009). The precision was slightly better for δ^2H than for $\delta^{18}O$ because the measurement of $^{18}O/^{16}O$ was more sensitive to varying room temperatures (Personal Communications with Los Gatos Company, 2009). For this reason, δ^2H values were primarily presented in this study where both $\delta^{18}O$ and δ^2H values did not have to be used.

3.4. Drainage delineation

Drainage above a gage or a sampling point was delineated using 30-m digital elevation model (DEM) following the standard procedure described in the ArcGIS 10.0 manual (ESRI Inc.). The 30-m DEM data were acquired from a USGS web site (http://seamless.usgs.gov; now https://www.usgs.gov/the-national-map-data-delivery/gis-data-download, access confirmed as of August 17, 2023). The geographic location of a gage or a sampling point was used as a pour point. After the delineation, the mean elevation for the drainage was calculated as arithmetic average of all raster grid elevations within the drainage.

4. Results

4.1. Hydrometeorology

Hydrologic conditions were very different in water years (October 1 in the previous year to September 30) 2006, 2007 and 2008 (all referring to water years or WY hereinafter; otherwise stated). Precipitation and snow depth were much higher in 2006 than in 2008 and particularly 2007 (Figures 2a and 2b). Annual precipitation was 1,247 mm, 1,472 mm, and 1,957 mm at Yosemite Valley, Wawona, and Gin Flat in 2006, respectively, compared to 568 mm, 631 mm, and 736 mm in 2007 (Figure 2a). Annual precipitation was 1,039 mm in 2008 at Wawona. The annual precipitation records in 2008 were incomplete at Yosemite Valley and Gin Flat. Precipitation primarily occurred from October to April or May each year, and little occurred during summer and

early fall (Figure 2a).
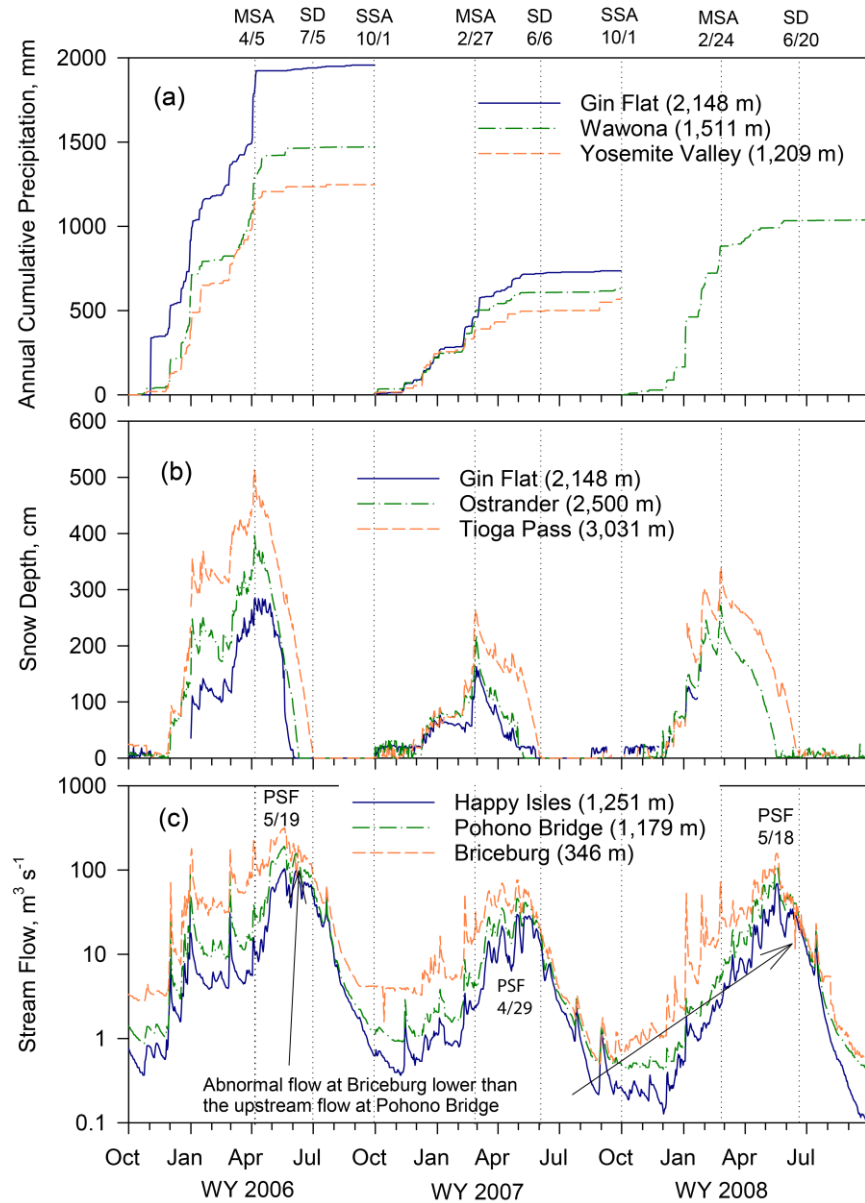
Figure 2. Hydrometeorology of the mid Merced River catchment for (a) daily accumulated precipitation, (b) daily snow depth, and (c) daily stream flow. Note the abnormal flow occasionally measured at Briceburg, which is lower than upstream flow at Pohono Bridge. Also note the lack of precipitation data in 2008 at Gin Flat and Yosemite Valley and snow depth data in most of 2008 at Gin Flat and in February 2008 at Tioga Pass. The grey dotted vertical grids mark the dates of the maximum snow accumulation (MSA), snow depletion (SD) at Tioga Pass, and start of snow accumulation (SSA) as October 1 each year; Dates of peak stream flow (PSF) were also marked in (c). Other than Gin Flat, the two other sites are not the same in (a) and (b), as precipitation and snow depth data were not available in the same sites.

Maximum snow accumulation occurred on April 5 in 2006, with a depth of 282 cm at Gin Flat, 396 cm at Ostrander and 514 cm at Tioga Pass (Figure 2b). The snowpack was depleted at the three sites by June 5, June 11 and July 5, respectively. Maximum snow accumulation occurred on February 27 in 2007, about 5 weeks earlier than in 2006, with maximum snow depths of 142, 192 and 264 cm at Gin Flat, Ostrander and Tioga Pass, respectively, approximately 50% of the depth in 2006. Snowpack depletion occurred in late May and early June of 2007 at all snow course sites. Snowpack reached a maximum depth on February 24 in 2008, similar to 2007, but with a much deeper snowpack (272 and 339 cm at Ostrander and Tioga Pass, respectively; Note that snow depth data was not available for most of 2008 at Gin Flat). Snowpack was mostly depleted by late May and June in 2008 at Ostrander and Tioga Pass, respectively.

The hydrograph in the Merced River follows a typical pattern of a snowmelt-dominated hydrologic system of the U.S. West, steadily increasing in early spring, peaked in mid spring or late spring and then gradually decreasing (Figure 2c). Peak stream runoff occurred on May 19 in 2006, measured at 103 and 191 m^3 s^{-1} at Happy Isles and Pohono Bridge, respectively. Peak flows higher than these values have been recorded only 13 times from 1916 to 2008 at the same gages. Peak flows occurred earlier in drier 2007 on April 29, with only 30 and 46 m^3 s^{-1} at Happy Isles and Pohono Bridge, respectively. Peak flows below these values have been recorded only 11 times from 1916 to 2008. The flow condition in 2008 was intermediate, with peak flows of 69 and 112 m^3 s^{-1} on May 18, 2008, at Happy Isles and Pohono Bridge, respectively. Several flow spikes usually occurred before the peak flow, apparently driven by rainfall events. The flows at Briceburg were occasionally lower than the upstream location at Pohono Bridge (Figure 2c), showing the occasional problems on flow measurements at Briceburg as mentioned earlier.

Based on the information above, a water year was divided into four periods to facilitate understanding the temporal variability of isotopic composition in stream water in the following sections. Four periods were: (1) snow accumulation period from October 1 (previous calendar year) to maximum snow accumulation (MSA) in spring at Tioga Pass; (2) snowmelt rising period from MSA to peak stream flow (PSF) at Happy Isles and Pohono Bridge; (3) snowmelt receding period from PSF to snow depletion (SD) at Tioga Pass; and (4) baseflow period from SD to September 30. Snow depletion dates at Tioga Pass were chosen in consideration of the entire mid Merced River catchment. Snow depleted several weeks earlier in lower elevations (e.g., Gin Flat) than Tioga Pass (Figure 2b). The snow depletion dates at Tioga Pass would be too late to mark the

end of snow cover for many small catchments, which are mostly located below 2,500 m - the upper limit of the snow-rain transition zone (Figure 1). However, snow at the observation sites melted out several weeks before the basin itself was free of snow (*Rice et al.*, 2011). In addition, snowpack was much deeper in higher elevations than lower elevations (Figure 2b) and the depletion of snowpack in the areas above Tioga Pass should occur much later than that at Tioga Pass. Therefore, using snow depletion dates at Tioga Pass to represent the entire mid Merced River catchment appears to be a balanced consideration following the rule of thumb.

4.2. Isotopic composition in precipitation, stream water and groundwater

Mean isotopic values varied significantly over locations in precipitation, stream water and groundwater and from precipitation to stream water and groundwater (Table 1). The mean δ^2H values ranged from -80.2 to -106.5‰ in snowpits excavated at the maximum snow accumulation in spring 2006 (Dana Lake samples not included) and in precipitation collected at NADP site from November 2006 to April 2007, with an elevation range of 1,393-2,500 m. The mean δ^2H values varied from -90.5‰ to -102.4‰ in stream water along the Merced River above Briceburg and from -64.2‰ to -101.3‰ in tributaries with a mean drainage elevation ranging from 913 m to 2,969 m. The mean δ^2H values in four springs varied between -67.6‰ and -99.0‰, with sampling locations ranging in elevation from 372 to 1,210 m, and between -80.4‰ and -94.1‰ in groundwater, with sampling ports ranging in elevation from 544 to 1,994 m.

Temporal variability of δ^2H values, as illustrated by 1σ values in Table 1, was the greatest in snow and precipitation, with 1σ ranging from 10.5‰ to 21.0‰, and generally the lowest in spring and groundwater, with $1\sigma < 3.0‰$ for most sites. The 1σ δ^2H value varied from 4.1‰ to 7.5‰ for stream water samples collected in the Merced River above Briceburg and $< 3.6‰$ for all tributaries except Yosemite Creek and the South Fork (8.8‰ and 7.0‰, respectively).

δ^2H values in snow and precipitation varied significantly between storms. δ^2H values in precipitation at NADP site in the Park ranged from -109.9‰ to -54.3‰ from November 2006 to April 2007 at an elevation of 1,393 m (Figure 3a). δ^2H values in snowpits at much higher elevations also changed significantly over depth, with a range of -126.8 to -72.6‰ at Badger Pass (elev. 2,226 m) and -159.4 to -71.6‰ at Ostrander (elev. 2,500 m) (Figure 3b and 3c). It was impossible in this study to associate the variation of δ^2H values over snow depth with storm history but nevertheless it approximately reflected the temporal changes of δ^2H values in snowfall over time.
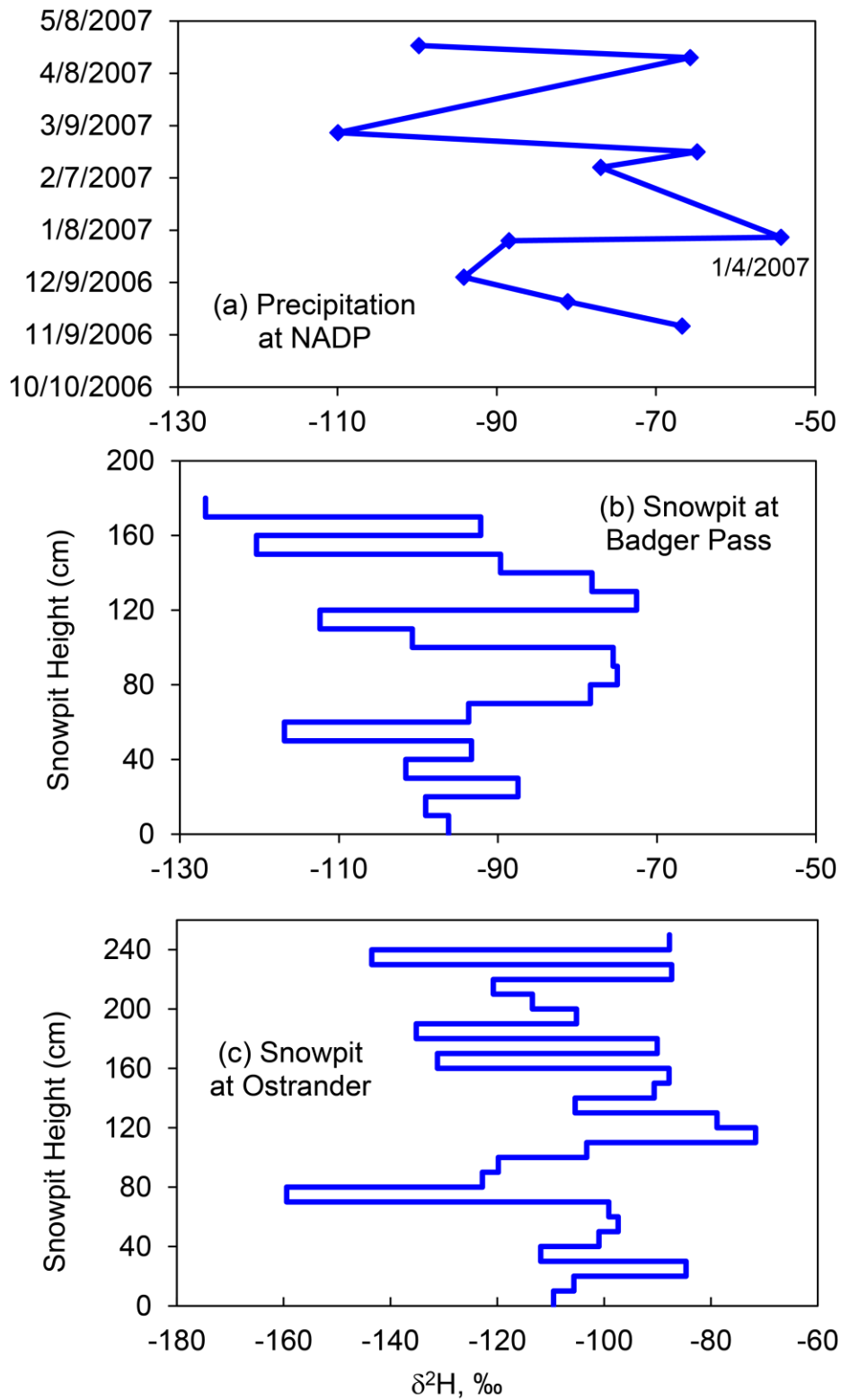
335

Figure 3. (a) Temporal variation of δ^2H in precipitation at the National Atmospheric Deposition Program (NADP) site located in Yosemite Valley; (b) and (c) δ^2H profiles in snowpits excavated at the maximum snow accumulation at Badger Pass and Ostrander, respectively.

δ²H values in stream water along the Merced River varied over time, with more depleted

340 (lower) values during the snowmelt period (snowmelt rising + receding periods) and more enriched values (higher) during the snow accumulation and baseflow periods (Figure 4). δ²H values in stream water along the Merced River became more enriched with an increase in drainage areas or a decrease in sampling elevations, with the lowest values at Happy Isles and the highest values at Briceburg consistently from 2006 to 2008 except for a couple of samples.

345
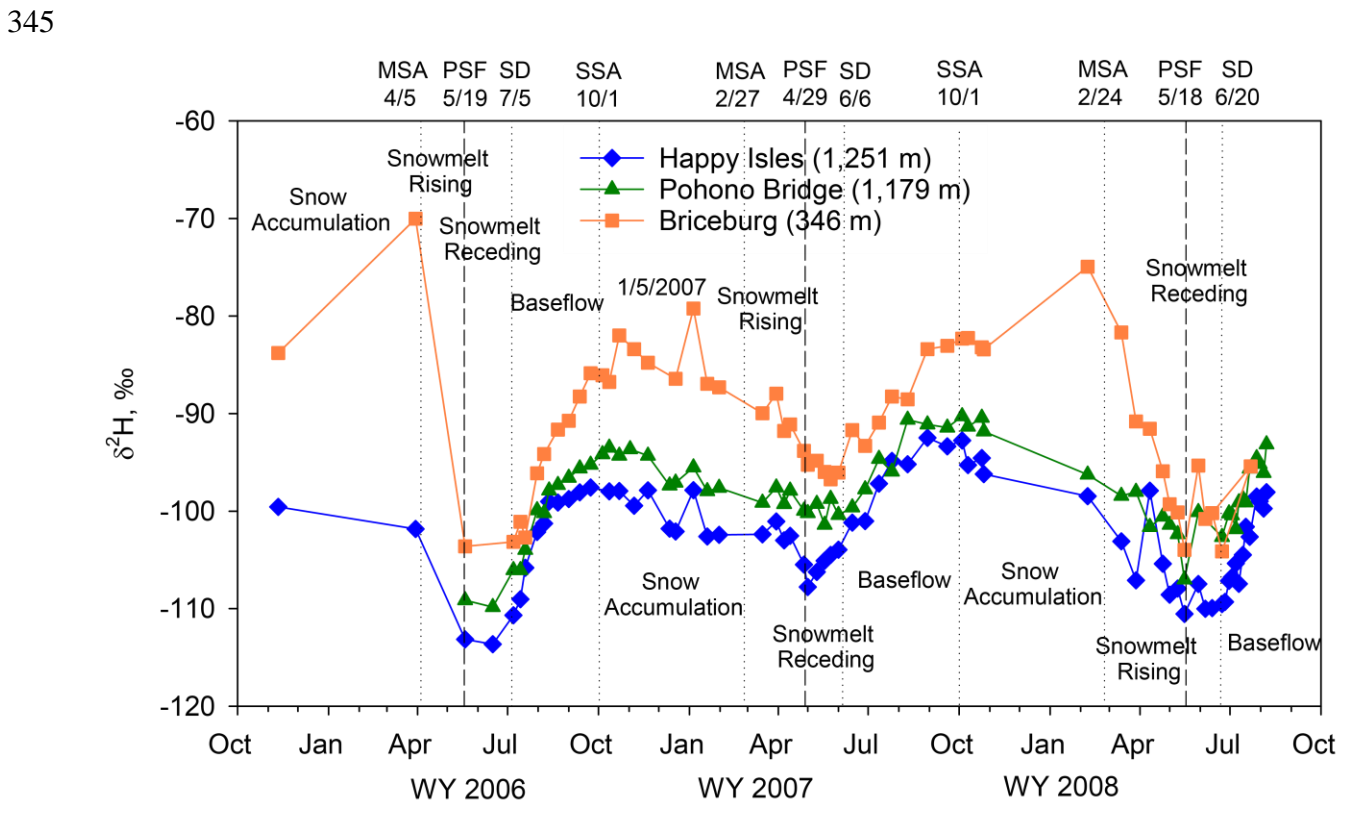
Figure 4. Variation of δ²H values in stream water from water years 2006 to 2008 at Happy Isles, Pohono Bridge and Briceburg. Dates marked by grey, dotted vertical grids are the same as in Figure 2 with addition of peak stream flow (PSF) with dashed lines. Four periods were also marked wherever space is allowed.

350

During the snow accumulation period, isotopic composition in the Merced River tended to become gradually depleted at Happy Isles, Pohono Bridge and Briceburg (Figure 4). For example, δ²H values were -98.0‰ on October 12, 2006, and -102.4‰ on January 31, 2007, at Happy Isles. There were isolated spikes in isotopic values during the period, e.g., a spike on January 5, 2007,

355 at all three gages and on February 8, 2008, at Briceburg. These isolated spikes appear to be caused by rain events with more enriched isotopic composition. For example, a major rain event occurred

on January 4, 2007, with 12 mm recorded at Yosemite Valley and δ^2H value of -54.3‰ at NADP site (Figure 3a), which increased stream flow (Figures 2c) and δ^2H values in stream water abruptly the next day at all three gages (Figure 4). During this period, δ^2H values decreased significantly (p

360 < 0.05) with an increase in stream flow by a logarithmic function at Happy Isles and Pohono Bridge, but increased significantly ($p < 0.05$) at Briceburg (Figure 5). The increase was apparently a result of greater rainwater inputs with more enriched isotopic signature. The magnitude of stream flow spikes was much higher at Briceburg than at the other higher elevation gages during the snow accumulation periods, suggesting much more rainfall inputs from lower elevations at Briceburg

365 (Figure 2c), causing an increase in isotopic values in stream water with an increase in stream flow.
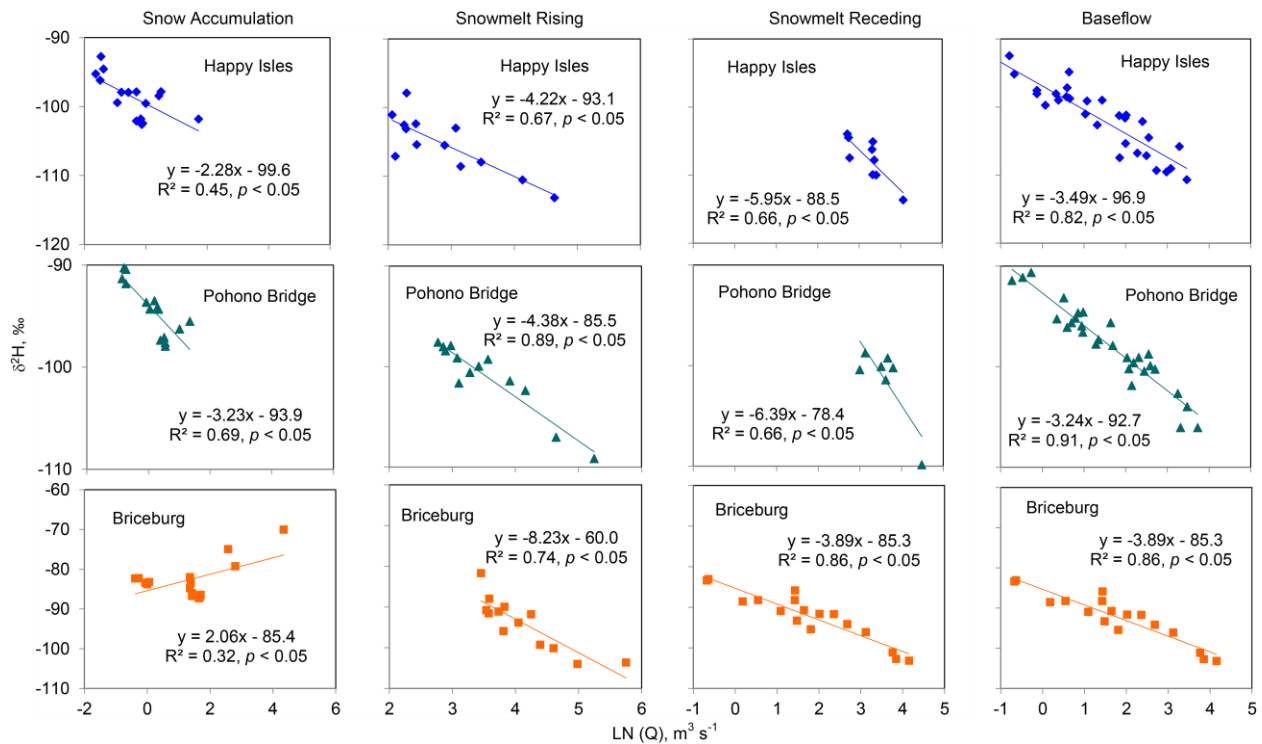
Figure 5. Correlation between δ^2H values in stream water and stream flow (natural logarithmic values) during four periods at Happy Isles, Pohono Bridge and Briceburg.

370

During the snowmelt period (snowmelt rising + receding periods), the variation of δ^2H values over time followed the shape of a trough (Figure 4). In fact, the variation can be described by a parabola function, particularly for 2006 and 2008 at Happy Isles (R^2 = 0.98 and 0.91, respectively; curves not shown). The lowest values, which occurred at peak flows, were

375   significantly inversely correlated with peak flows ($R^2 = 1.0$, $n = 3$, $p < 0.05$) and varied over years, e.g., -113.7‰ in 2006, -107.8‰ in 2007 and -110.6‰ in 2008 at Happy Isles. During the period, isotopic composition became depleted with an increase in stream flow ($p < 0.05$), consistent between the snowmelt rising and receding periods for all three Merced River gages (Figure 5).

During the baseflow period, isotopic composition became enriched over time (Figure 4).
380   The isotopic enrichment over time during this period occurred much more rapidly (steeper slopes) than the isotopic depletion during the snow accumulation period. Also, the enrichment was much stronger at Briceburg (again steeper slopes) than at Happy Isles and Pohono Bridge, particularly in 2006 and 2007. During the period, δ^2H values decreased with an increase in stream flow significantly ($p < 0.05$) at all three Merced River gages (Figure 5).

385

4.3. Local meteoric water line and local evaporation line in stream water and groundwater

A local meteoric water line (LMWL) of δ^2H versus $\delta^{18}O$ was established using 71 snow and rain samples collected at NADP site and snowpits (each 10-cm snow sample treated as an individual sample for this purpose) excavated at Badger Pass, Gin Flat, and Ostrander (Figure 6a).
390   The slope and intercept of the LMWL were 7.88 and 9.39 ($R^2 = 0.96$, $p < 0.001$), respectively, which are very close to those (8 and 10, respectively) of the global meteoric water line (GMWL) of *Craig* (1961).

Most stream water samples collected along the Merced River and its tributaries fall near LMWL on the δ^2H-$\delta^{18}O$ plot (Figures 6b and 6c). However, the slopes of δ^2H-$\delta^{18}O$ linear trends
395   for individual sites were lower than that of LMWL and varied over locations (Table 2), indicating an evaporation effect. The slope was lower than 6.13 for all Merced River locations, with the intercept less than -14.7. For tributaries, the slope and intercept were even lower, e.g., slope < 5.0 in seven of eight tributaries and intercept mostly less than -30.0 (Table 2). R^2 values varied from 0.73 to 0.90 for all Merced River locations except Cascade Picnic Area (0.48), but were lower than
400   0.76 for all tributaries except Yosemite Creek (0.95) and the South Fork (0.94).

Almost all Merced River samples collected during the snow accumulation period are located right below the LMWL (Figure 6b), showing a local evaporation line (LEL) with a slope of 7.29 and an intercept of -0.72 ($n = 81$, $R^2 = 0.93$) (Table 2). Merced River samples collected during the snowmelt rising period are scattered near LMWL except for one outlier on lower left of
405   LMWL (Figure 6b), with a slope of 6.08 and an intercept of -15.34 ($n = 75$, $R^2 = 0.77$) for LEL

(Table 2). During the snowmelt receding period, most samples were below LMWL (Figure 6b) and the slope and intercept of LEL were 6.61 and –9.19 ($n = 50$, $R^2 = 0.73$), respectively (Table 2). During the baseflow period, all samples other than a few were below LMWL (Figure 6b) and the slope and intercept of LEL were 6.00 and –18.58 ($n = 134$, $R^2 = 0.89$), respectively (Table 2). The samples, highlighted in an orange rectangle box on Figure 6b, were further away from LMWL and collected in the Merced River at Briceburg and the South Fork confluence during the baseflow period.
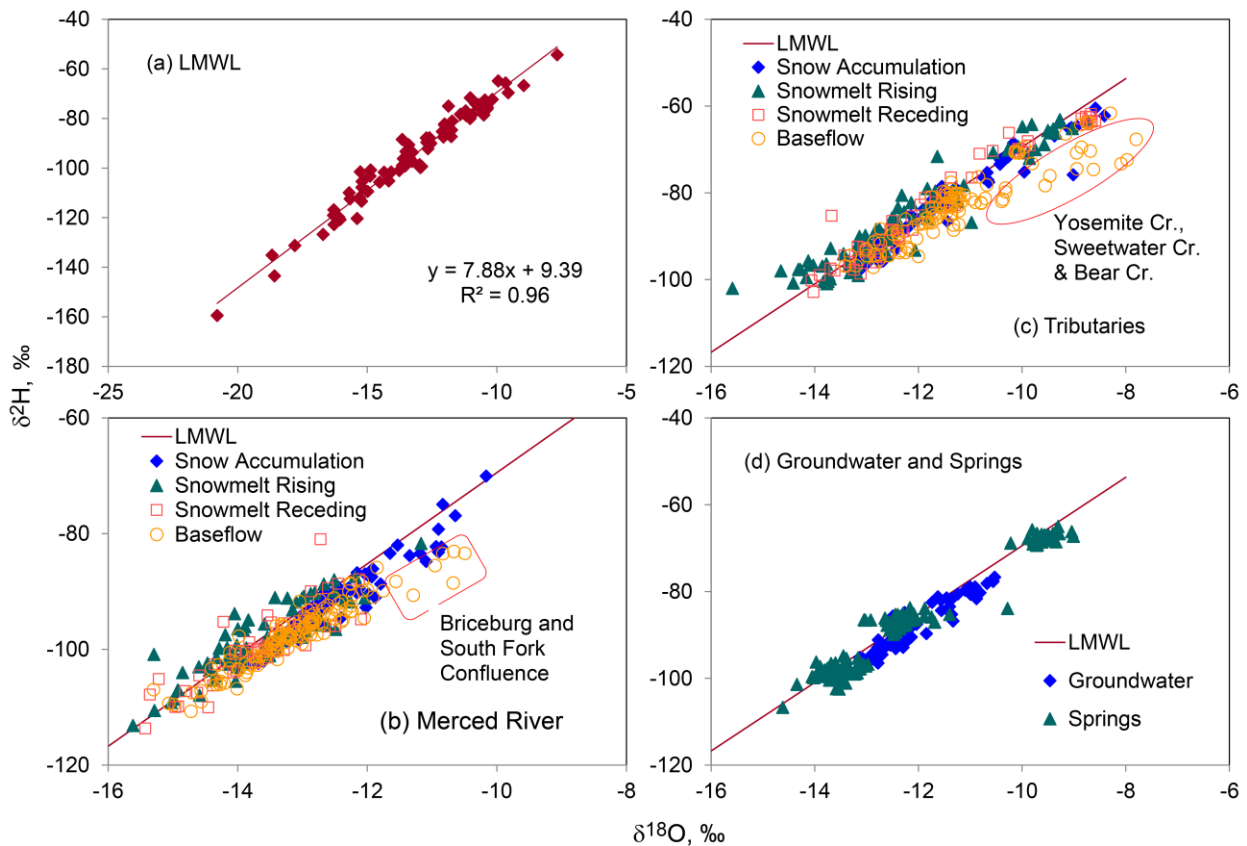
Figure 6. Relationship between δ^2H and $\delta^{18}O$ values in (a) precipitation (rain and snow); and stream water samples collected during four periods defined in Figure 4 for (b) Merced River at all locations listed in Table 1; (c) all tributaries listed in Table 1; and (d) groundwater and spring water collected at all sites.

Compared to the Merced River, the result of tributaries by periods was somewhat different. Other than the baseflow period (particularly those circled by an orange oval), samples are scattered more closely around LMWL during all periods (Figure 6c). The slope of LEL was greater than 7.0 and noticeably higher than those of the Merced River (Table 2). The intercept was also higher,

ranging from -0.19 to 3.52 and R^2 values were higher than 0.92. During the baseflow period, the slope and intercept were significantly lower, 5.85 and -17.29, respectively, with an R^2 of 0.83, which was primarily attributed to samples collected in Yosemite Creek, Sweetwater Creek and Bear Creek at extremely low flows (circled in Figure 6c). It is the baseflow samples that caused the lower slopes for individual catchments than those during the other three periods (Table 2).

Table 2. Local meteoric water line (LMWL), local evaporation line (LEL), and isotopic composition at the intersection of LEL and LMWL.

	Sample Number	Mean Catchment Elevation (m)	Local Evaporation Line			Intersection of LEL & LMWL	
			Slope	Intercept	R^2	$\delta^{18}O$ (‰)	δ^2H (‰)
Precipitation for LMWL	71		7.88	9.39	0.96		
Merced River by Catchment							
Happy Isles	68	2743	5.64	-24.31	0.90	-15.0	-109.0
El Capitan	49	2624	5.51	-25.07	0.89	-14.5	-105.0
Pohono Bridge	64	2580	5.69	-22.11	0.86	-14.4	-103.9
Cascade Picnic Area	37	2539	4.27	-37.75	0.48	-13.0	-93.4
El Portal	35	2483	4.94	-31.63	0.73	-13.9	-100.5
South Fork Confluence	33	2350	4.56	-34.51	0.78	-13.2	-94.8
Briceburg	54	2067	6.13	-14.70	0.84	-13.7	-98.7
Merced River by Period (Samples from all catchments together)							
Snow Accumulation	81		7.29	-0.72	0.93	-17.0	-125.0
Snowmelt Rising	75		6.08	-15.34	0.77	-13.7	-98.7
Snowmelt Receding	50		6.61	-9.19	0.73	-14.6	-105.6
Baseflow	134		6.00	-18.58	0.89	-14.9	-107.7
Tributaries by Catchment							
Tenaya Creek	43	2528	3.20	-53.93	0.57	-13.5	-97.3
Yosemite Creek	50	2516	4.67	-33.35	0.95	-13.3	-95.5
Bridalveil Creek	48	2232	4.31	-35.18	0.76	-12.5	-88.9
Cascade Creek	38	2228	4.95	-25.52	0.61	-11.9	-84.4
Crane Creek	37	1621	3.92	-34.94	0.75	-11.2	-78.8
South Fork	40	1857	5.56	-19.42	0.94	-12.4	-88.2
Sweetwater Creek	32	1058	1.95	-50.49	0.24	-10.1	-70.2
Bear Creek	29	913	3.40	-33.47	0.61	-9.6	-66.0
Tributaries by Period (Samples from all catchments together)							
Snow Accumulation	71		7.47	3.52	0.93	-14.2	-102.6
Snowmelt Rising	82		7.01	-0.19	0.92	-11.0	-77.1
Snowmelt Receding	59		7.32	2.47	0.94	-12.3	-87.5
Baseflow	105		5.85	-17.29	0.83	-13.1	-94.1
Springs (All)	148		7.55	4.76	0.95	-13.8	-99.8
Groundwater (All)	59		7.22	-0.83	0.86	-15.3	-111.2

Note that the last four tributaries listed in Table 1 were not inlcuded here because their δ^2H-$\delta^{18}O$ relationship was not significnat ($p > 0.05$) due to the lack of samples. Also, see text for discussion about the division of four periods for a water year. All R^2 values are significant with $p < 0.01$. Both δ^2H and $\delta^{18}O$ values at the intersection of LEL and LMWL were mathematically determined by finding the solution of sumiltaneous equations of LEL and LMWL.

The δ^2H-$\delta^{18}O$ relation in groundwater and springs were closer to LMWL than in stream water (Figure 6d and Table 2). The slope and intercept of the evaporation lines were 7.22 and -0.83 for groundwater and 7.55 and 4.76 for spring water, respectively.

435

4.4. Variation of isotopic values in stream water, groundwater and precipitation with elevation

Mean isotopic values of stream water from relatively small catchments (8-122 km^2; including all listed under tributaries in Table 1 except the South Fork), groundwater, and rock glacier outflows were highly correlated with mean elevations of their catchment areas (Figure 7a and 7b). The slope and intercept were -0.0022 and -7.57 for $\delta^{18}O$ (R^2 = 0.91, n = 16, $p < 0.001$), respectively, and -0.019 and -48.7 for δ^2H (R^2 = 0.96, n = 16, $p < 0.001$). The Crane Flat and Hodgdon Meadow wells are located near the mid Merced River divide (inside and outside, respectively) and far away from major streams (Figure 1). Groundwater in these wells was deemed to be derived from precipitation in the drainage area above each well. These drainage areas, along with the mean drainage elevations, were computed the same as for a stream sampling location using well locations as pour points. The result indicates that elevations vary narrowly from the well locations to the drainage summit at Crane Flat and Hodgdon Meadow, with a relief of only 33 and 429 m, respectively (Table 1). A similar analysis cannot be performed for the other groundwater wells due to the complex topography and their proximity with the Merced River and thus samples from those wells were excluded in this analysis.

Variation of isotopic values in snow with sampling elevation was examined using mean isotopic values from four snowpits excavated along an elevation gradient and a rain gage located at Yosemite Valley (Figure 7a and 7b). The slope of the δ^2H-elevation linear relationship was identical to that of small streams, groundwater, and rock glacier outflows and the intercept was also very close (-51.3 versus -48.7), even though its R^2 value was much lower (R^2 = 0.74, n = 5, p = 0.06).

An analysis was also conducted to exclude samples of two groundwater wells and three rock glacier outflows outside the mid Merced River catchment (Figure 7c). The result indicated that the δ^2H-elevation relationship did not change significantly, with a slope of -0.016 and intercept of -52.5 (R^2 = 0.94, n = 11, $p < 0.001$).

To examine if evaporation affected the isotope-elevation relationship, the mean isotopic

values in stream water were corrected using both LMWL and LEL (Table 2). Using the isotopic values at the intersection between LMWL and LEL, the isotope-elevation relationship was still

465 significant for small streams ($R^2 = 0.96$ for δ^2H, $n = 7$, $p < 0.001$) and yielded a similar slope (-0.017) and intercept (-50.5) (Figure 7d).
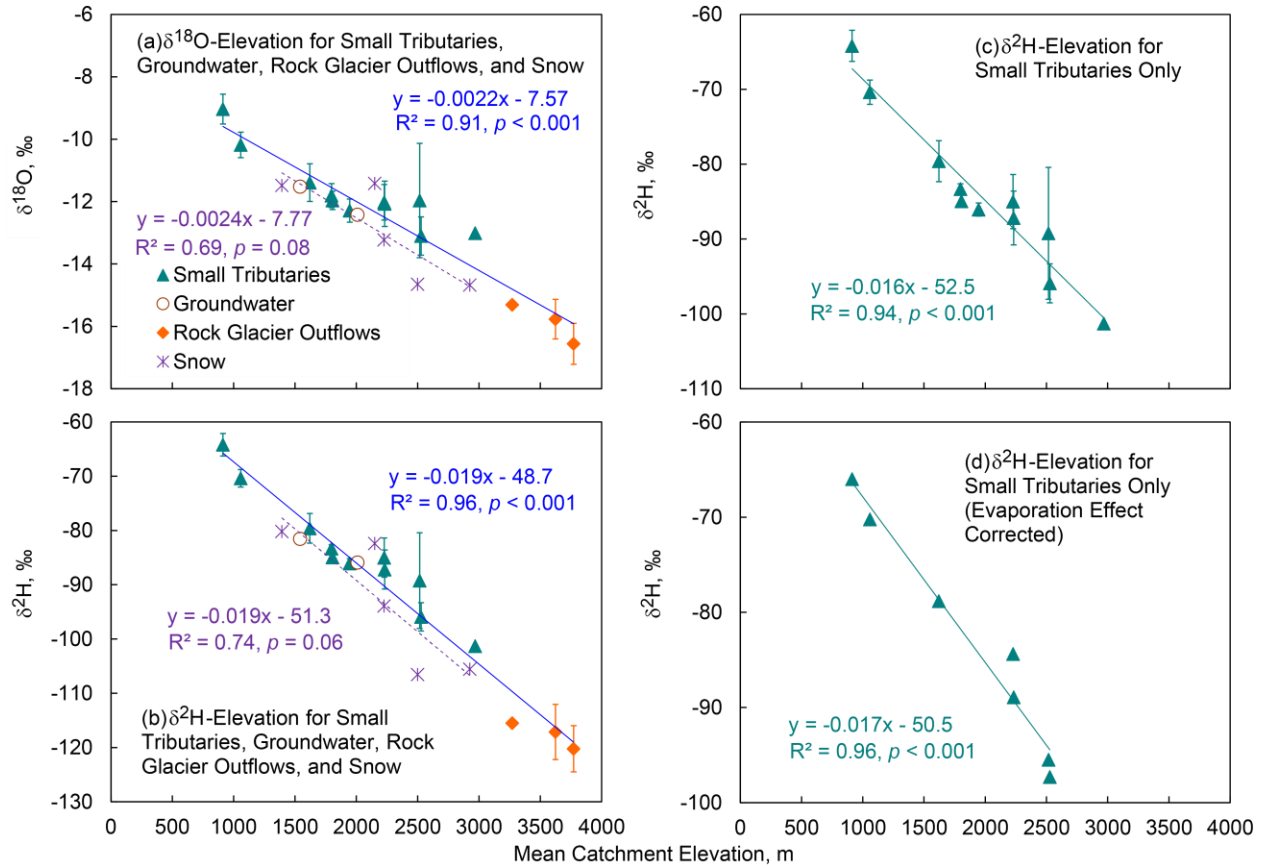
Figure 7. Variation of isotopic composition with mean catchment elevations: (a) and (b) for $\delta^{18}O$ and δ^2H
470 values, respectively, in small tributaries (catchment area < 122 km^2), groundwater with estimated source water elevations (Crane Flat and Hodgdon Meadow), and rock glacier outflows, along with snow and rain samples. The blue solid line shows the linear trend for small tributaries, groundwater and rock glacier outflows and the dashed purple line for snow and rain samples. (c) for δ^2H values in small tributaries without groundwater and rock glacier outflows; and (d) for δ^2H values in small tributaries with evaporation effect
475 corrected by local meteoric water line. The number of samples in (d) is less than in (c) due to the lack of samples to establish a significant relationship between δ^2H and $\delta^{18}O$ values for the last four tributaries listed in Table 1.

Seasonal variation of the δ^2H-elevation relationship was examined using samples collected in small tributaries, groundwater and rock glacier outflows during the four periods defined earlier

480   (Figure 8). The slopes and intercepts of δ^2H-elevation linear relationship did vary over the periods, but not remarkably. The slope varied between -0.015 and -0.021 and the intercept values between -40.3 and -55.0 for all these periods except the snow accumulation period and the snowmelt rising period in 2006. Samples were not collected in tributaries in spring and summer of 2006 and the samples collected in the snow accumulation period in 2006 did not cover a wide range of

485   elevations. The slope and intercept did not appear to change significantly from the snowmelt rising period to the snowmelt receding period in 2007 and 2008. Merced River samples were also plotted independently in Figure 8. It is apparent that Merced River samples collected over seasons did closely follow the trend of small tributaries, groundwater and rock glacier outflows.
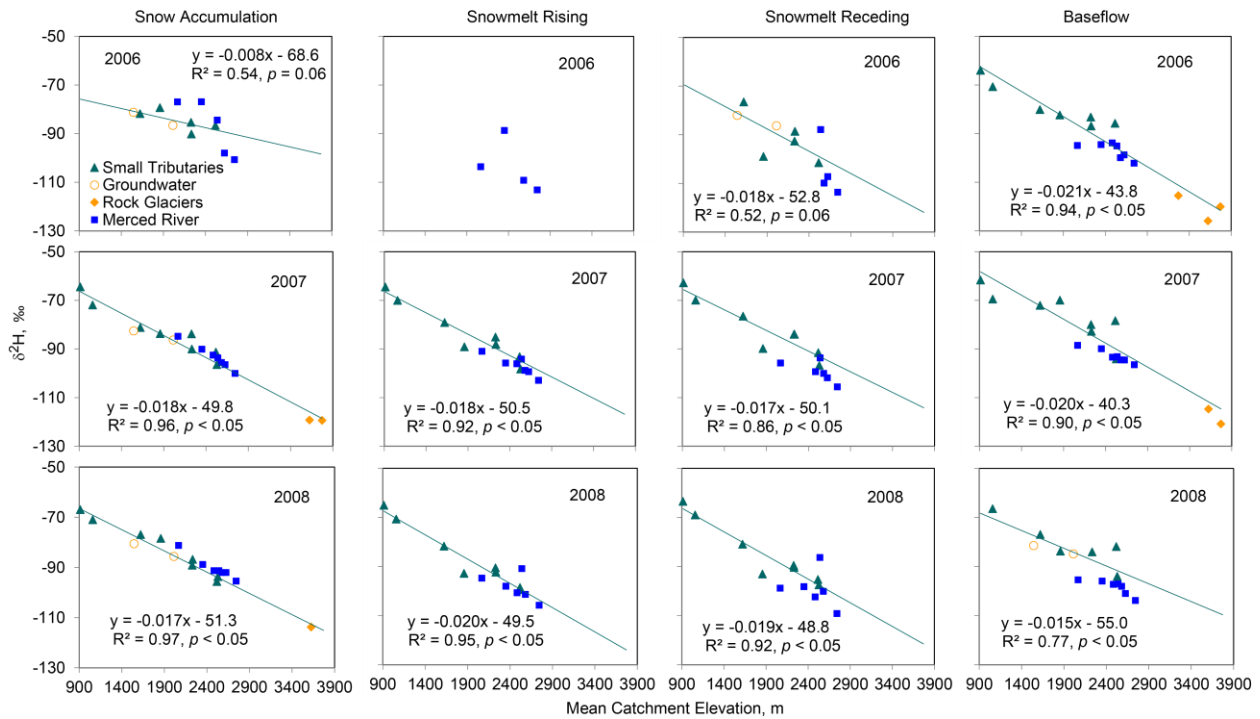
490

Figure 8. Seasonal variation of the δ^2H-elevation relationship in small tributaries, groundwater and rock glacier outflows, with a linear trend (green). Samples from Merced River were also plotted, but not included in establishing the trend line. Four periods were defined the same as Figure 4. The number of samples for each analysis varies depending on the availability of samples. Note that no samples were available for

495   tributaries, groundwater and rock glacier outflows during the snowmelt rising period in 2006 due to the road blockage caused by a massive land slide.

5. Discussion and application

5.1. Controls on isotopic composition in stream water and groundwater

5.1.1. Elevation effect

Elevation exerts a major control on the mean isotopic values in stream water at small catchments (including rock glacier outflows) and groundwater in the mid Merced River catchment (Figures 7a and 7b), which is consistent with *Jeelani et al.* (2010). Unlike monsoon precipitation samples collected along an elevation gradient in India (*Kumar et al.*, 2010), the slopes and intercepts of their correlations did not vary much over seasons and years with dramatically different hydrologic and climatic conditions (Figure 8). The elevation gradient determined by those samples, e.g., -0.22‰/100m for $\delta^{18}O$ and -1.9‰/100m for δ^2H on average (Figures 7a and 7b), essentially represents lapse rate of isotopic composition in meteoric water in the mid Merced River catchment. This lapse rate is corroborated with the lapse rate for temperature and caused by Rayleigh distillation as the heavier isotopes are concentrated in the precipitation, resulting in clouds progressively becoming isotopically lighter with ascending to higher elevations or moving further away from ocean (*Poage and Chamberlain*, 2001; *Clark and Fritz*, 1997). The mean lapse rate of this study is reasonably close to that obtained elsewhere around the world, which averaged to be -0.28‰/100m for $\delta^{18}O$ as reviewed by *Poage and Chamberlain* (2001). The lapse rate of $\delta^{18}O$ is identical to that of precipitation in a south Ecuadorian montane cloud forest catchment (San Francisco catchment, 1,800-2,800 m) (*Windhorst et al.*, 2013) and almost the same as that of precipitation in the upper Heihe River in the northwestern China (1,674-5,103 m), where a gradient of -0.18‰/100m was obtained (*Wang et al.*, 2009b). It is also very close to the gradient in northern California, where δ^2H values in groundwater changed from -40‰ to -120‰ from the coast to the Sierra crest with a relief of 4,000 m, with a lapse rate of -2.0‰/100m (*Ingraham and Taylor*, 1991). Since the isotopic lapse rate did not change longitudinally in Sierra Nevada (*Friedman and Smith*, 1970), this lapse rate may be applicable to the western slope of the entire Sierra Nevada.

However, this lapse rate is significantly lower than that (-4‰/100 m for δ^2H) reported earlier by *Friedman and Smith* (1970) using snow-core samples collected around April 1 of 1969 in the west slope of Sierra Nevada. The lapse rate of *Friedman and Smith* (1970) also does not agree with the result of our snow samples (Figures 7a and 7b). The discrepancy in the results between our snow samples and those of *Friedman and Smith* (1970) is primarily caused by significant temporal variability of isotopic composition in snowpack over seasons and years and

530   uneven temporal variation over elevation bands as found by *Jodar et al.* (2016) for the European Alps. For example, δ^2H value in a snowpit at Gin Flat (elevation = 2,150 m) was -103‰ reported by *Friedman and Smith* (1970) but -81.5‰ in this study, with a difference of 21.5‰. δ^2H value was -139‰ at Big Whitney Meadow (elevation = 2,970 m) in 1969, whereas it was -105.5‰ at similar elevation (2,926 m) at Dana Lake in 2006, with even a greater difference than at Gin Flat

535   at 33.5‰. It was very wet in 1969, with annual precipitation of 1,649 mm compared to 1,247 mm in 2006 at Yosemite Valley. Information on snowfall amount or snow depth in 1969 was not available, but heavier storms usually result in lighter stable isotopes in snow (*Ingraham*, 1998). In addition, snow is usually subject to isotopic fractionation if sublimation and melting occur (*Taylor et al.*, 2001; *Earman et al.*, 2006; *Frisbee et al.*, 2009; *Earman et al.*, 1996). *Dettinger et al.* (2004)

540   demonstrated that melting and sublimation did occur in the snowpack in Sierra Nevada before April 1. It is not possible to evaluate how significant isotopic fractionation has affected the isotopic composition in the snow samples collected by *Friedman and Smith* (1970), as $\delta^{18}O$ was not analyzed in their study. However, the isotopic composition in the snow samples of this study, which was mostly collected at the maximum accumulation, was very close to GMWL of *Craig*

545   (1961) (Figure 6a), indicating that isotopic fractionation effect due to sublimation was not evident in our snow samples.

        Using samples from precipitation, the lapse rate may vary significantly over years and seasons and is not always reliable (*Hemmerle et al.*, 2021). *Gamboa et al.* (2022) demonstrated that the lapse rate of δ^2H varied from -1.4 to -3.5‰/100m using precipitation samples collected

550   during intermittent periods from 1984 to 2017 in the Atacama Desert of the Northern Chile. From the same study, the lapse rate of δ^2H was -1.6‰/100m using groundwater samples and the mean sub-basin elevations, which is very close to ours. Furthermore, the lapse rate may vary dramatically with different climates, particularly when precipitation samples are used. For example, the lapse rate of δ^2H was -0.8‰/100m (summer) and -0.9‰/100m (winter) in the arid and semi-arid Tucson

555   Basin in the Southern Basin-and-Range Province of Arizona and New Mexico (*Eastoe and Wright*, 2019), -0.7‰/100m in the humid Great Lakes region in the Eastern Democratic Republic of the Congo (*Balagizi et al.*, 2018), and -3.4‰/100m in the Juncal River basin of Central Chile (2,200-3,000m) (*Ohlanders et al.*, 2013).

560

5.1.2. Evaporation effect

All samples of the Merced River, tributaries, groundwater and spring water were very close to LMWL in the δ^2H-δ^{18}O bivariate plots exempt for some collected during the baseflow period (Figure 6). The slopes of the local evaporation lines in groundwater and spring water were only slightly lower than that of LMWL (Table 2), indicating that evaporation during groundwater recharge was not very strong. However, the slopes of LEL in the Merced River and tributaries were noticeably lower than that of LMWL (Table 2), showing an apparent evaporation effect, the same as *Jeelani et al.* (2013) and *Reckerth et al.* (2017).

Both the slope and R^2 values of LEL were generally lower in tributaries than in the Merced River except for R^2 values at Yosemite Creek and the South Fork when LELs were constructed using data from individual catchments (Table 2). The lower slopes in tributaries were primarily caused by samples collected during low flows in later summer and fall, particularly those with waterfalls such as Yosemite Creek and wider but shallower channels such as the South Fork (Figure 6c). When all samples were grouped into four periods, the slopes and R^2 values of LEL in tributaries became much higher and closer to LMWL than those in the Merced River during all periods other than the baseflow period (Table 2). Apparently, evaporation was stronger in the Merced River than in tributaries during all periods other than the baseflow period. During the baseflow period, stronger evaporation occurred in tributaries, particularly in Yosemite Creek (Figure 6c). However, the isotope-elevation relation established using small tributaries and groundwater was not strongly affected by evaporation and the isotopic composition in the Merced River was still primarily controlled by source waters from various elevations even during the baseflow period (Figure 8).

5.1.3. Snowmelt and isotopic fractionation effects

The temporal variability of isotopic values in snow was much higher than that of stream water (Figures 3 and 4; Table 1). Isotopic composition in stream water over three water years with very different precipitation amounts has attenuated much of the temporal variability of stable isotopes in precipitation, consistent with the observation of *Kendall and Coplen* (2001), *Dutton et al.* (2005), *Jeelani et al.* (2013), and *Reckerth et al.* (2017). The variability attenuation primarily explains why the isotope-elevation relations did not vary dramatically when stream samples were used (Figure 8). Compared to the variability of isotopic composition in groundwater and spring

water, however, the isotopic composition in stream water still varied significantly over seasons (with respect to 1σ values in Table 1). During snowmelt, δ^2H values in stream water at Happy Isles, Pohono Bridge and Briceburg were much lower than during the other periods (Figure 4). This result was apparently caused by the snowmelt contribution to streams from melting snowpack, supported by *Shaw et al.* (2014) and *Liu et al.* (2017). However, the seasonality did not significantly change the slopes of δ^2H-elevation relationship over seasons (Figure 8). Also, δ^2H values in stream water were consistently distinct from 2006 to 2008 over sampling locations at Happy Isles, Pohono Bridge and Briceburg, except for a few samples that were affected by rainfall events (Figure 4). It is suggested that even during snowmelt, elevation still exerts a major control on the isotopic composition in stream water in the mid Merced River catchment.

Studies have shown that snowmelt becomes isotopically enriched over time due to isotopic fractionation between ice and liquid water (e.g., *Taylor et al.*, 2001; *Earman et al.*, 2006). As a result, isotopic values in snowmelt from a snowmelt lysimeter were significantly lower than those in the bulk snowpack before the peak snowmelt and higher after that, resulting in a monotonic curve with isotopic values gradually increasing over time in snowmelt and stream water (*Liu et al.*, 2004). The variation of δ^2H values during the snowmelt period in the Merced River followed a parabola curve (the curve not shown but the trend can be seen in Figure 4), instead of a monotonic one. In addition, the difference between the snowmelt rising and receding periods was not evident for δ^2H-flow relationship, δ^2H-$\delta^{18}O$ relationship, and δ^2H-elevation relationship (Figures 5, 6, and 8). These results suggest that isotopic fractionation between ice and liquid water in snowmelt did not appear to affect much the isotopic signature of stream water at the catchment scales involved in this study.

5.2. Applications and implications

The lapse rate of stable isotopes (or the isotope-elevation relation) in meteoric water acquired by this study would be useful for paleoelevation studies as demonstrated for Sierra Nevada of California by *Mulch et al.* (2006) and the Himalaya by *Hren et al.* (2009). This information is also very useful for understanding source waters (e.g., *Jean-Baptiste et al.*, 2022; *Jeelani et al.*, 2013) and the sensitivity of stream flow in response to climate change. For the latter, for example, stream flow during the baseflow period at lower elevations (e.g., Briceburg of this study) is more strongly affected by rainfall and thus more sensitive to changes in snow-rain ratio

in the future as alluded by Figure 5 and the relevant text in section 4.2. Below are two additional examples of its applications in watershed hydrology and hydrometeorology.

625

5.2.1. Building conceptual understanding on hydrometeorologic processes

Based on the discussion in section 5.1, a catchment characteristic isotopic value (CCIV) of source waters – isotopic composition at the mean catchment elevation that represents source waters from the entire catchment - can be defined by the isotope-elevation relation for all sub-catchments

630 in the mid Merced River catchment (Figure 9). This characteristic value was simply calculated by the isotopic value-elevation function using the arithmetic mean of catchment elevations. In combination with local meteoric water line, CCIV helps elucidate hydrometeorologic processes over seasons. In the Merced River at Happy Isles, for example, δ^2H value was below CCIV starting on March 30, 2006, and near CCIV again on August 7, 2006, after a trough-shape turn (Figure 9a).

635 These two dates approximately match the start and end of the snowmelt season for 2006 based on stream flow. The start date was also very close to the maximum snow accumulation date (Figures 2b and 9a). The end date was about four weeks later than the snow depletion date at Tioga Pass, which is consistent with *Rice et al*. (2011) that snow at the observation sites melted out several weeks before the catchment itself was free of snow. Therefore, the end date also appears to match

640 the end of snowmelt. The snowmelt duration determined this way in 2007 and 2008 also agrees reasonably well with that determined by stream flow. Similarly, the results from Pohono Bridge and Briceburg (not shown) are consistent with Happy Isles. The intersection of CCIV line and the isotopic time series curve marks reasonably well the snowmelt duration. Since isotopic values are highly correlated with stream flows (Figure 5), in addition, the lowest isotopic value during the

645 snowmelt period can be used to infer the relative magnitude of snowmelt event. The lower the isotopic value at the bottom of trough the higher the magnitude of snowmelt event. This approach seems to be a powerful tool to determine the duration and relative magnitude of snowmelt events for ungagged basins without stream flow measurements.

In the Merced River at Happy Isles, δ^2H values were above CCIV line during the baseflow

650 periods and below the line during the snow accumulation periods (Figure 9a), reflecting the shift of source water elevations, evaporation and occasional rainfall effects as discussed earlier. The local meteoric water line and evaporation line of groundwater could be used to assist in differentiating the dominant processes during these periods. For example, δ^2H values were 5-8‰

more enriched during the baseflow period in 2007 than in 2006 (Figure 9a). The enrichment for these samples is deemed to be primarily caused by evaporation, rather than shift in source water elevation. These samples collected in 2007 are located below and further to the right of LMWL and LEL of groundwater than the samples collected in 2006 (Figure 10a), indicating a stronger evaporation effect. Though the shift in source water elevation and evaporation cannot be quantitatively determined, the CCIV line helps build a conceptual understanding of hydrometeorologic processes.
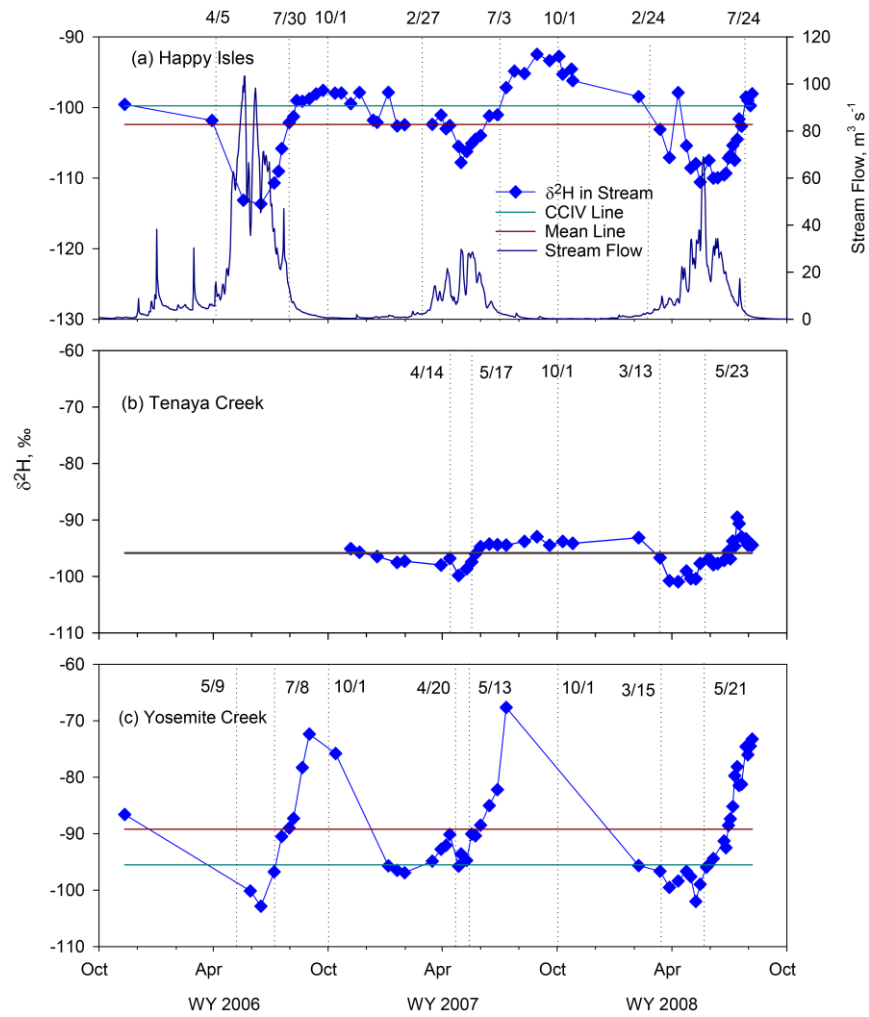
Figure 9. δ^2H values in stream water in (a) Merced River at Happy Isles, with stream flow, (b) Tenaya Creek, and (c) Yosemite Creek, along with catchment characteristic isotopic value (CCIV) of δ^2H and a line determined by mean δ^2H value in samples. Dates in (a) mark the start and end of snowmelt season determined by hydrograph at Happy Isles and October 1; dates on (b) and (c) mark the start and end of snowmelt season using the intersections of the time series curve and CCIV. Note that the mean and CCIV lines overlap in (b).
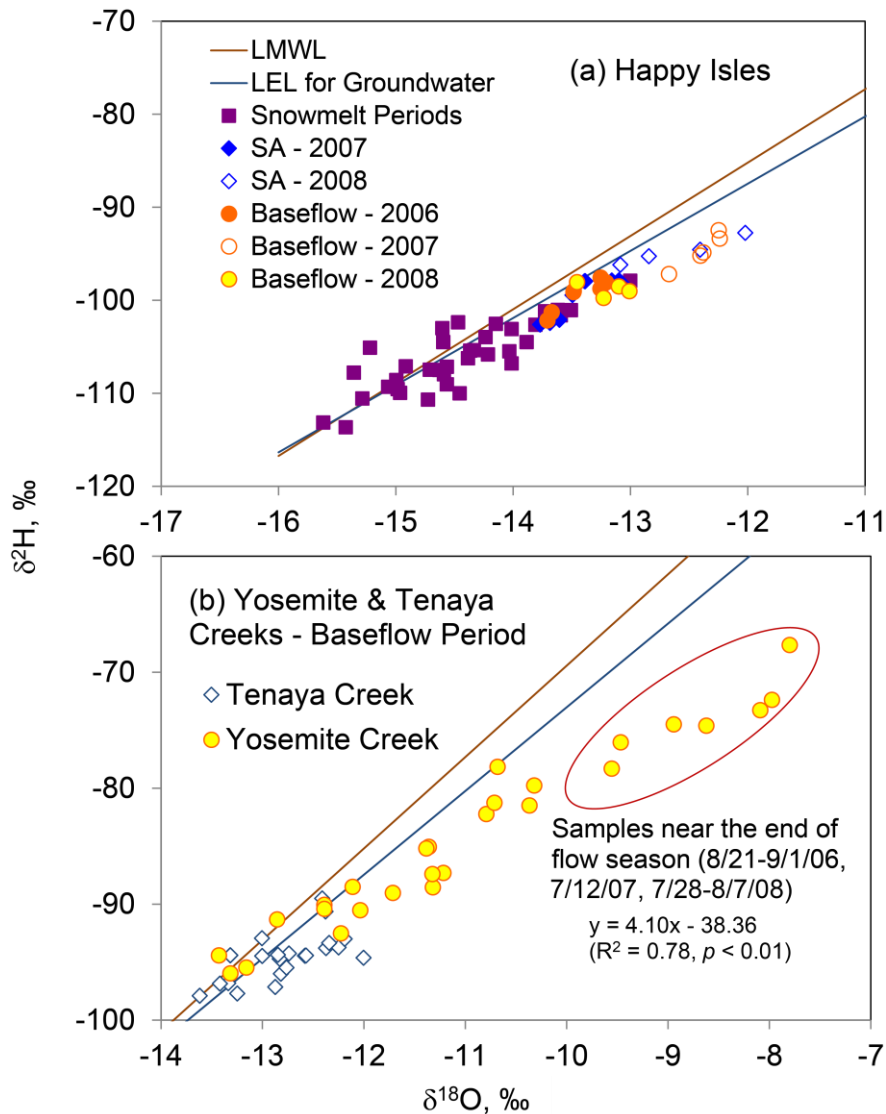
Figure 10. Scatter plot of δ^2H vs. $\delta^{18}O$ for (a) Merced River at Happy Isles during different periods and (b) comparison between Tenaya Creek and Yosemite Creek during the baseflow period. Local meteoric water line (LMWL) and evaporation line (LEL) of groundwater are also shown as references. Highlighted by a red oval are samples collected in Yosemite Creek near the end of flow seasons from 2006 to 2008, along with a linear regression equation (Samples collected in Teneya Creek near the end of flow seasons at Yosemite Creek did not have a significant relationship ($R^2 = 0.09$, $p = 0.47$) between δ^2H and $\delta^{18}O$).

Comparing the temporal variation of δ^2H values relative to the CCIV line between Yosemite Creek and Tenaya Creek, two ungauged streams, reveals more interesting results (Figures 9b and 9c). The two adjacent basins share many similarities, e.g., basin area, elevation ranges, and mean basin elevations (Table 1 and Figure 1), other than Yosemite Creek terminating

680   with two cascading waterfalls (739 m tall) in Yosemite Valley. Indeed, the lowest δ^2H values were

close and occurred at about the same time, indicating that peak snowmelt occurred with similar

magnitudes at about the same time in these catchments. The dates when the CCIV line and time

series curve intersected were similar, suggesting that the duration of snowmelt events appear to be

close as well. However, the variation of δ^2H values relative to the CCIV line was very different,

685   with most samples particularly those collected in the baseflow periods far above the line in

Yosemite Creek (Figures 9b and 9c). Compared to Tenaya Creek, the samples collected near the

end of flow seasons from 2006 to 2008 in Yosemite Creek were plotted far below and further right

to LMWL and LEL of groundwater, with a slope of 4.10 ($R^2 = 0.76$, $p < 0.01$) (Figure 10b). The

samples collected at Tenaya Creek during the same periods did not have a significant relationship

690   for δ^2H-$\delta^{18}O$, likely due to relatively small changes among samples compared with the analytical

accuracy, particularly of $\delta^{18}O$. Nevertheless, this result indicates that evaporation was much

stronger in Yosemite Creek than in Tenaya Creek and shifting of source water toward lower

elevations was not the main reason. It is suggested that Yosemite Creek is much more sensitive to

climate warming than Tenaya Creek. Flow in Yosemite Creek was intermittent in drier years (e.g.,

695   it dried up starting mid-July in 2007). Without even considering any effect of other factors (e.g.,

shift in snow-rain ratio and the earlier onset of snowmelt), an increase in air temperature alone

would increase evaporation, reduce flow, and further shorten the duration of flow in Yosemite

Creek. This trend is certainly not good news for Yosemite National Park tourists as Yosemite Falls

are one of the most attractive features in the park.

700   One would argue that a simple horizontal line using the arithmetic mean isotopic value

from samples collected in the same catchment could serve the same purpose as the CCIV line. The

mean line could work if the number of samples was large enough and evaporation was known to

be neglectable *a priori* such as Tenaya Creek (Figure 9b). However, it would not work for

catchments with strong evaporation such as Yosemite Creek. Since the arithmetic mean line is

705   about 5‰ above the CCIV line in Yosemite Creek (Figure 9c), the duration and magnitude of

snowmelt events will be much exaggerated and evaporation effect will be greatly under-stated.

           Based on the above analysis, a guideline is developed to identify hydrometeorologic

processes using the time series of stable isotopes and the CCIV line for the mid Merced River

catchment, which we think applicable to other snowmelt-fed catchments. If isotopic values in

710   stream water are on or near the CCIV line, it indicates that source waters of stream flow are likely

from all elevations, with an approximately equal discharge rate from higher and lower elevations. If the isotopic values are far below the line, stream water during the period is dominated by source waters from snowmelt and perhaps from higher elevations as well. If the isotopic values are far above the line, stream water likely experiences strong evaporation or a shift in source waters to lower elevations.

5.2.2. Determining mean elevations of source waters for springs and groundwater

Information on recharge areas of springs and groundwater is paramount for the protection of their quantity and quality (*e.g., Yanggen and Born*, 1990) and for the assessment of climate change effect (*Taylor et al.*, 2013), but usually remains unknown in most catchments (e.g., *Chen et al.*, 2004) or a challenge (*Koeniger et al.*, 2017). Using the isotope-elevation relation (Figure 7), the mean elevations of source waters (recharges) were calculated for springs and groundwater in the mid Merced River catchment (Figure 11), following the same approach as *Jeelani et al.* (2010). For example, the mean source water elevation for Fern Spring was 2,035 m based on its mean δ^2H values in Table 1 and the equation shown in Figure 7b. This calculation was verified by 30-m DEM using a GIS. The geographic location of Fern Spring was used as a pour point to delineate a drainage area following the same procedure as for groundwater at Hodgdon Meadow and Crane Flat. The mean catchment elevation determined with DEM is 2,108 m for Fern Spring (its catchment ranging in elevation from 1,199 m to 2,277 m). The difference in the mean catchment elevation between the two methods is only 73 m, which is less than 1σ value determined by the isotope-elevation relation (Figure 11). The mean source water elevation for Drinking Fountain, which was calculated to be 1,014 m by the isotopic approach, can also be verified anecdotally. Drinking Fountain (372 m) is located between Sweetwater Creek and Bear Creek in the low mountain areas (Figure 1). The mean drainage elevation determined by DEM is 1,058 m for Sweetwater Creek and 913 m for Bear Creek, which are slightly higher and lower, respectively, than the mean source water elevation of Drinking Fountain determined by the isotope method. These results demonstrate the reliability of the isotopic method and further validate the isotope-elevation relationship established using small streams, rock glacier outflows, and groundwater, as these sites were not included in the analysis of isotope-elevation relationship.

Based on the δ^2H-elevation relation, the mean source water elevation for springs at Happy Isles and Fen in Yosemite Valley is higher than 2,500 m, approximately 1,500 m above their

resurfacing (sampling) locations (Figure 11). The mean source water elevation is close to 2,500 m for deep wells in Yosemite Valley and to 2,000 m for shallow wells at El Portal. The mean source water elevations for these springs and groundwater are around the present and future threshold

745 elevations (2,181 m for 1995-2004 and 2,486 m for 2085-2094 in Sierra Nevada) determined by *Scalzitti et al.* (2016), below which the variability of snowpack is primarily determined by temperature and above which by precipitation. The source waters of these springs and groundwater will likely be subject to the impact of both temperature increase and precipitation pattern change in the future.

750
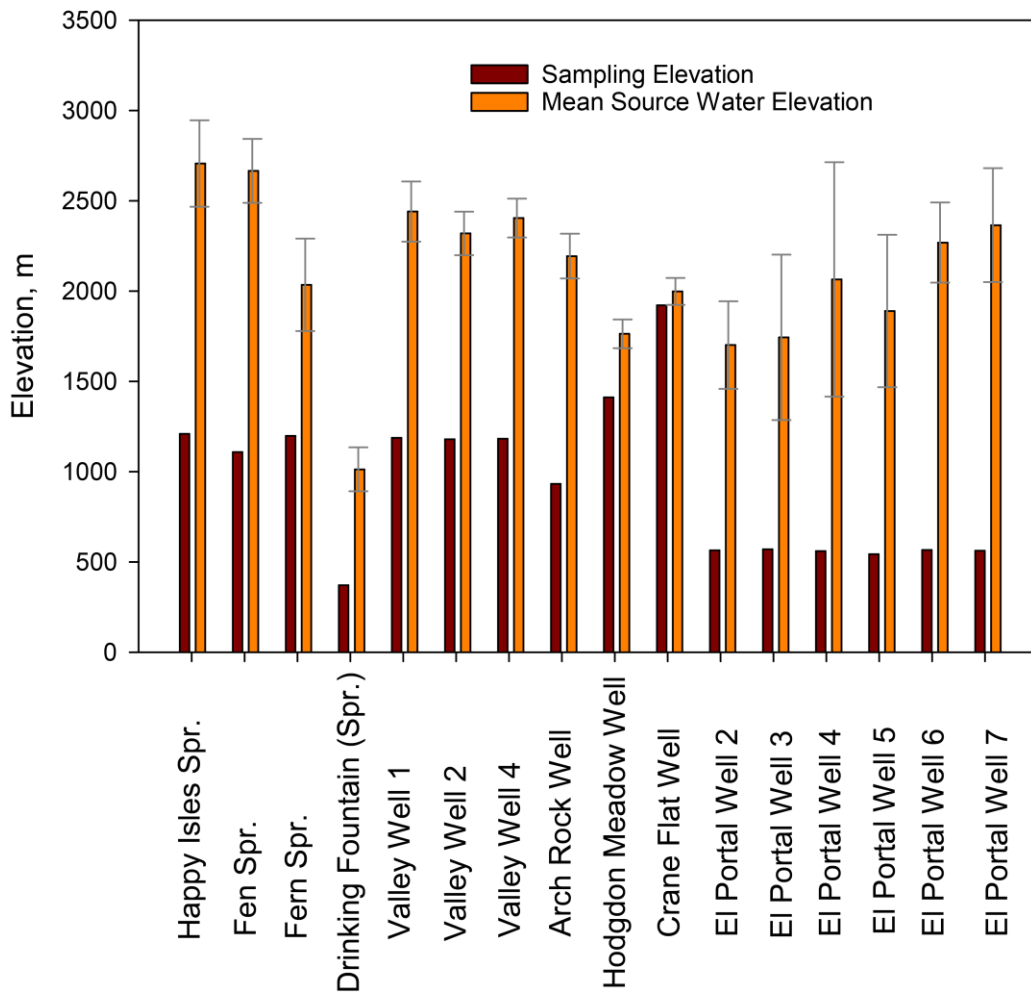
Figure 11. Mean elevations of recharge areas for springs and groundwater calculated by δ^2H-elevation relation, along with 1σ standard deviations and sampling elevations.

These springs, including Fern Spring, one of the most attractive touring sites in the valley,
755 could be negatively impacted by the shift in snow-rain proportion in the future as their recharge

areas are centered in the upper snow-rain transition zone. So do the groundwater storage and water table dynamics in both Yosemite Valley and El Portal. However, the response is certainly more sensitive in the valley than in El Portal as the source water area of groundwater in the valley extends from ~1,180 m (where wells are located) to > 2,500 m, with more areas located in the snow-covered area than the source water area of groundwater in El Portal (which extends from < 500 m to > 2,000 m).

Note that the estimated source water (recharge) elevations for groundwater in the valley and El Portal refer to elevations where water originated. The path ways of source waters, e.g., whether via direct underground flow paths as of the case in *Frisbee et al.* (2013) or by mixing of groundwater recharge and river water as suggested by *Shaw* et al., (2014), cannot be elucidated by stable isotopic data alone but can be done by combining isotopes and geochemical tracers as demonstrated by *Liu et al.* (2004). Unlike *Adomako et al.*, (2010), in addition, the recharge rates of groundwater and spring water cannot be determined due to the lack of a lapse rate of runoff depth with elevation in our study. However, the recharge elevation ranges do help improve our understanding of the sensitivity of climate change impact on groundwater recharge.

6. Conclusions

Stable isotopic composition of stream water and groundwater is strongly controlled by elevations of source waters in the mid Merced River catchment, with an average isotopic lapse rate of -1.9‰/100m for δ^2H and -0.22‰/100m for δ^{18}O in meteoric water. This lapse rate, determined by small streams, groundwater and rock glacier outflows, is more robust than the one established earlier using snow samples collected in Sierra Nevada. Temporal variability of isotopic compositions in stream water and groundwater was significantly attenuated compared to that in precipitation. Evaporation had little effect on isotopic signature of precipitation, spring water, and groundwater, but affected stream water particularly during low flows in summer and fall. The isotopic composition of stream water was most depleted during the snowmelt periods, as a result of significant contributions of snowmelt runoff. However, the isotope-elevation relation was not significantly affected by evaporation and snowmelt effects, nor by isotopic fractionation between ice and liquid water in snowmelt. The isotopic composition in stream water in the Merced River consistently becomes more enriched with decreasing sampling elevations (or increasing in drainage area) for all seasons. Using the isotope-elevation relation, a catchment characteristic

isotopic value (CCIV) was established based on the mean drainage elevation. CCIV, in combination with local meteoric water line and local evaporation line, helps elucidate the hydrometeorologic processes at different stages or seasons and the sensitivities of stream flow in response to climate warming. The analysis suggests that Yosemite Creek is most sensitive to climate warming due to strong evaporation associated with waterfalls. It is also suggested that evaporation effect on stream flow must be considered in understanding how climate change impacts stream flow. Based on the isotope-elevation relation, it was determined that groundwater in the valley is from drainage areas centered in the upper snow-rain transition zone (2,000–2,500 m). It is suggested that groundwater (including spring water) in the valley is very vulnerable to the shift in snow-rain ratio. Continuous and frequent monitoring of changes in stable isotopes in stream water and groundwater along an elevation gradient is a very powerful tool in watershed hydrology for major snowmelt-fed river systems in the region such as the U.S. West, which will greatly help advance our understanding of how stream flow responds to temperature rise and shift in snow-rain ratio.

Author contribution

FL and MC designed the experiments and FL and GS carried them out. FL performed data analyses and developed all figures and tables. FL prepared the manuscript with contributions from all co-authors.

Competing interests

The authors declare that they have no conflict of interest.

Data availability

The isotopic data used in this study will be available to the public through CUASHI data repository site. Authors are working on the task and a DOI will be provided by the time of acceptance.

Acknowledgements

The authors thank Dr. Robert Rice and Dr. Peter Kirchner for taking rock glacier outflow samples, Katy Warner at the Yosemite National Park for taking precipitation samples, and Denise Melendez for processing meteorological data and analyzing samples. Two undergraduate students, Dannique Aalbu from the University of California, Merced and Clifford Tonsberg Jr. from the University of Tennessee, helped sampling in summer 2008, supported by the NSF's Research Experience for Undergraduates (REU) program. Funding was primarily provided by California Energy Commission through Public Interest Environmental Research (No. 500-02-004) and Dr. Martha Conklin's start-up fund at the University of California, Merced and Dr. Fengjing Liu's start-up fund from Michigan Technological University. The Research was also supported in part by the National Science Foundation, through the Southern Sierra Critical Zone Observatory (EAR-0725097 and EAR1331939), and the USDA-NIFA Capacity Building Grant Program (#2011-38821-30956 and #2013-38821-21461) and two Evans-Allen Grants (#0225140 and #1007239).

References

Adomako, D., Maloszewski, P., Stumpp, C., Osae, S., and Akiti, T. T.: Estimating groundwater recharge from water isotope (δ^2H, δ^{18}O) depth profiles in the Densu River basin, Ghana, *Hydrological Sciences Journal*, 55:8, 1405-1416, DOI: 10.1080/02626667.2010.527847, 2010.

Araguas-Araguas, L., Froehlich, K., and Roozanski, K.: Deuterium and oxygen-18 isotope composition of precipitation and atmospheric moisture, *Hydrol. Process.*, 14, 1341-1355, 2000.

Balagizi, C. M., Kasereka, M. M., Cuoco, E., and Liotta, M.: Influence of moisture source dynamics and weather patterns on stable isotopes ratios of precipitation in Central-Eastern Africa, *Science of the Total Environment*, 628-629: 1058-1078, https://doi.org/10.1016/j.scitotenv.2018.01.284, 2018.

Bateman, P. C.: Plutonism in the Central Part of the Sierra Nevada Batholith, California, USGS Professional Paper 1483, 186pp, 1992.

Berman, E. S., Gupta, M., Gabrielli, C., Garland, T., and McDonnell, J. J.: High-frequency filed-deployable isotope analyzer for hydrological applications, *Water Resources Research*, 45, W10201, doi:10.1029/2009WR008265, 2009.

Cayan, D. R., Kammerdiener, S. A., Dettinger, M. D., Caprio, J. M., and Peterson, D. H.: Changes

850 in the onset of spring in the western United States, *Bulletin of the American Meteorological Society*, 82 (3), 399-415, 2001.

Chen J. S., Li, L., Wang, J. Y., Barry, D. A., Sheng, X. F., Gu, W. Z., Zhao, X., and Chen, L.: Water resources: Groundwater maintains dune landscape, *Nature*, 432, 459-460, doi:10.1038/432459a, 2004.

855 Clark, I. and Fritz, P.: *Environmental Isotopes in Hydrogeology*, CRC Press, pp. 328, 1997.

Clow, D. W., Mast, M. A., and Campbell, D. H.: Controls on surface water chemistry in the Upper Merced River Basin, Yosemite National Park, California, *Hydrological Processes*, Vol. 10, 727-746, 1996.

Craig, H.: Isotopic variations in meteoric waters, *Science*, 133, 1702-1703, 1961.

860 Dettinger, M. D., Cayan, D. R., Meyer, M. K., and Jeton, A. E.: Simulated hydrologic responses to climate variations and changes in the Merced, Carson, and American River basins, Sierra Nevada, California, 1900-2099, *Climatic Change*, 62, 283-317, 2004.

Dutton, A., Wilkinson, B. H., Welker, J. M., Bowen, G. J., and Lohmann, K. C.: Spatial distribution and seasonal variation in $^{18}O/^{16}O$ of modern precipitation and river water

865 across the conterminous USA, *Hydrological Processes*, 19, 4121-4146, 2005.

Earman, S., Campbell, A. R., Phillips, F. M., Newman, B. D.: Isotopic exchange between snow and atmospheric water vapor: Estimation of the snowmelt component of groundwater recharge in the southwestern United States, Journal of Geophysical Research: Atmospheres, 111(D9), doi:1029/2005JD006470, 2006.

870 Earman, S. and Dettinger, M.: Potential impacts of climate change on groundwater resources: a global review, J. Water Clim. Change, http://dx.doi.org/10.2166/wcc.2011.034, 2011.

Eastoe, C. J. and Wright, W. E.: Hydrology of Mountain Blocks in Arizona and New Mexico as Revealed by Isotopes in Groundwater and Precipitation, *Geosciences*, 9 (461), http://dx.doi.org/10.3390/geosciences9110461, 2019.

875 Fayad, A., Gascoin, S., Faour, G., Lopez-Moreno, J. I., Drapeau, L., Le Page, M., Escadafal, R.: Snow hydrology in Mediterranean mountain regions: A review, Journal of Hydrology, 551, 374-396, 2017.

Friedman, I. and Smith, I. S.: Deuterium content of snow cores from Sierra Nevada area, *Science*, Vol. 169, 467-470, 1970.

880   Friedman, I., Harris, J. M., Smith, G. I., and Johnson, C. A.: Stable isotope composition of waters in the Great Basin, United States 1. Air-mass trajectories, *Journal of Geophysical Research*, VOL. 107, NO. D19, 4400, doi:10.1029/2001JD000565, 2002.

Frisbee, M. D., Phillips, F. M., Campbell, A. R., and Hendrickx, J. M. H.: Modified passive capillary samplers for collecting samples of snowmelt infiltration for stable isotope
885   analysis in remote, seasonally inaccessible watersheds 1: laboratory evaluation, *Hydrological Processes*, 24(7), 825-833, DOI: 10.1002/hyp.7523, 2010.

Frisbee, M. D., Phillips, F. M., Campbell, A. R., Liu, F., and Sanchez, S. A.: Streamflow generation in a large, alpine watershed in the southern Rocky Mountains of Colorado: Is streamflow generation simply the aggregation of hillslope runoff responses? *Water Resources*
890   *Research*, 47, W06512, doi: 10.1029/2010WR009391, 2011.

Gamboa, C., Godfrey, L., Urrutia, J., Herrera, C., Lu, X., and Jordan, T.: Conditions of groundwater recharge in the hyperarid southern Atacama Desert, *Global and Planetary Change*, 217: 103931, https://doi.org/10.1016/j.gloplacha.2022.103931, 2022.

Gat, J. R.: Oxygen and hydrogen isotopes in the hydrologic cycle, *Annual Review of Earth and*
895   *Planetary Sciences*, 24, 225-262, 1996.

Gutenberg, B., Buwalda, J. P., and Sharp, P.: Seismic explorations on the floor of Yosemite Valley, California, Bull. Geol. Soc. Am., 67(8), 1051–1078, doi:10.1130/0016-7606(1956)67, 1956.

Hemmerle, H., van Geldern, R., Juhlke, T. R., Huneau, F., Garel., E., Santoni, S., and Barth, J. A.
900   C.: Altitude isotope effects in Mediterranean high-relief terrains: a correction method to utilize stream water data, Hydrological Sciences Journal, VOL. 66, NO. 9, 1409–1418, https://doi.org/10.1080/02626667.2021.1928672, 2021.

Howat, I. M., and Tulaczyc, S.: Trends in California's snow-water volume over a half century of climate warming, *Annuals of Glaciology*, 40: 151-156, 2005a.

905   Howat, I. M., and Tulaczyc, S.: Climate sensitivity of spring snowpack in the Sierra Nevada, *Journal of Geophysical Research – Earth Surface*, 110, F04021, doi:10.1029/2005JF000356, 2005b.

Hren, M. T., Bookhagen, B., Blisniuk, P. M., Booth, A. L., and Chamberlain, C. P.: $\delta^{18}O$ and δD of streamwaters across the Himalaya and Tibetan Plateau: Implications for moisture

910   sources and paleoelevation reconstructions, *Earth and Planetary Science Letters*, 288, 20-32, 2009.

Hunsaker, C. T., Whitaker, T. W., and Bales, R. C.: Snowmelt runoff and water yield along elevation and temperature gradients in California's southern Sierra Nevada, Journal of the American Water Resources Association, 1-12, DOI: 10.1111/j.1752-1688.2012.00641.x, 915   2012.

Ingraham, N. L.: Isotopic variations in precipitation, in: *Isotope Tracers in Catchment Hydrology*, edited by: Kendall, C. and McDonnell, J. J., Elsevier Science B. V., Amsterdam, pp. 839, 1998.

Ingraham, N. L. and Taylor, B. E.: Light stable isotope systematics of large-scale hydrologic 920   regimes in California and Nevada, *Water Resources Research*, 27(1), 77-90, 1991.

Jeelani, G., Bhat, N. A., and Shivanna, K.: Use of δ^{18}O tracer to identify stream and spring origins of a mountainous catchment: A case study from Liddar watershed, Western Himalaya, India, *Journal of Hydrology*, 393: 257-264, http://dx.doi.org/10.1016/j.jhydrol.2010.08.021, 2010.

925 Jeelani, G., Kumar, U. S., and Kumar, B.: Variation of δ^{18}O and δD in precipitation and stream waters across the Kashmir Himalaya (India) to distinguish and estimate the seasonal sources of stream flow, *Journal of Hydrology*, 481: 157-165, http://dx.doi.org/10.1016/j.jhydrol.2012.12.035, 2013.

Jean-Baptiste, J., Le Gal Salle, C., and Verdoux, P.: Water stable isotopes and volumetric 930   discharge rates to monitor the Rhone water's seasonal origin, *Heliyon*, 6, https://doi.org/10.1016/j.heliyon.2020.e04376, 2020.

Jodar, J., Custodio, E., Lamban, L. J., Herrera, C., Martos-Rossilo, S., Sapriza, G., and Rigo, T.: Correlation of the seasonal isotopic amplitude of precipitation with annual evaporation and altitude in alpine regions, *Science of the Total Environment*, 550: 27-37, 935   http://dx.doi.org/10.1016/j.scitotenv.2015.12.034, 2016.

Kendall, C., and Coplen, T. B.: Distribution of oxygen-18 and deuterium in river waters across the United States, *Hydrological Processes*, 15, 1363-1393, 2001.

Kendall, C. and McDonnell, J. J. (Eds): *Isotope Tracers in Catchment Hydrology*, Elsevier Science B. V., Amsterdam, pp. 839, 1998.

940 Knowles, N., Dettinger, M. D., and Cayan, D. R.: Trends in snowfall versus rainfall in the Western United States, *Journal of Climate*, 19, 4545-4559, 2006.

Koeniger P, Margane A, Abi-Rizk J, Himmelsbach T.: Stable isotope-based mean catchment altitudes of springs in the Lebanon Mountains, *Hydrological Processes*, 31:3708–3718, https://doi.org/10.1002/hyp.11291, 2017.

945 Kumar, B., Rai, S. P., Saravana Kumar, U., Verma, S. K., Garg, P., Vijaya Kumar, S. V., Jaiswal, R., Purendra, B. K., Kumar, S. R., and Pande, N. G.: Isotopic characteristics of Indian precipitation, *Water Resour. Res.*, 46, W12548, doi:10.1029/2009WR008532, 2010.

Liu, F., Williams, M. W., and Caine, N.: Sources waters and flow paths in an alpine catchment, Colorado Front Range, USA, *Water Resources Research*, Vol. 40, W09401, doi: 950 10.1029/2004WR003076, 2004.

Liu, F., Conklin, M. H., and Shaw, G. D.: Insights into hydrologic and hydrochemical processes based on concentration-discharge and end-member mixing analyses in the mid-Merced River Basin, Sierra Nevada, California, *Water Resources Research*, 53, doi:10.1002/2016WR019437, 2017.

955 Mast, M.A. and Clow, D. W.: Environmental characteristics and water quality of Hydrologic Benchmark Stations in the western United States, 1963-95: U.S. Geological Survey 1173-D, 114 p, 2010.

Melsen, L. A., Teuling, A. J., van Berkum, S. W., Torfs, P. J. J. F., and Uijlenhoet R.: Catchments as simple dynamical systems: A case study on methods and data requirements for 960 parameter identification, *Water Resources Research*, 50, 5577–5596, doi:10.1002/2013WR014720, 2014.

Mote, P. W., Hamlet, A. M., Clark, M. P., and Lettenmaier, D. P.: Declining mountain snowpack in western North America, *Bull. Ameri. Meteor. Soc.*, Vol. 86, 1-39, 2005.

Mulch, A., Graham, S. A., and Chamberlain, C. P.: Hydrogen isotopes in Eocene river gravels and 965 paleoelevation of the Sierra Nevada, *Science*, Vol. 313, 87-89, 2006.

O'Driscoll, M. A., DeWalle, D. R., McGuire, K. J., and Gburek, W. J.: Seasonal [18]O variations and groundwater recharge for three landscape types in central Pennsylvania, USA, *Journal of Hydrology*, 303, 108-124, 2005.

Ohlanders, N., Rodriguez, M., and McPhee, J.: Stable water isotope variation in a Central Andean
watershed dominated by glacier and snowmelt, *Hydrol. Earth Syst. Sci.*, 17, 1035–1050,
doi:10.5194/hess-17-1035-2013, 2013.

Peng, T. R., Huang, C. C., Chen, C. T., Chen, J. E., and Liang, W. J.: Using stable hydrogen and
oxygen isotopes to reveal monsoonal and related hydrological effects on meteoric water in
the Western Pacific monsoon region: A case study of the Ilan region, northeastern Taiwan,
Journal of Asian Earth Sciences, 128: 105-115,
http://dx.doi.org/10.1016/j.jseaes.2016.06.024, 2016.

Penna, D., Engel, M., Mao, L., Dell'Agnese, A., Bertoldi, G., and Comiti, F.: Tracer-based analysis
of spatial and temporal variations of water sources in a glacierized catchment, *Hydrol.
Earth Syst. Sci.*, 18, 5271–5288, doi:10.5194/hess-18-5271-2014, 2014.

Penna, D., Engel, M., Bertoldi, G., and Comoti, F.: Towards a tracer-based conceptualization of
meltwater dynamics and streamflow response in a glacierized catchment, *Hydrol. Earth
Syst. Sci.*, 21, 23–41, doi:10.5194/hess-21-23-2017, 2017.

Poage, M. A. and Chamberlain, C. P.: Empirical relationships between elevation and the stable
isotope composition of precipitation and surface waters: Consideration for studies of
paleoelevation change, *American Journal of Science*, Vol. 301, 1-15, 2001.

Reckerth, A., Stichler, W., Schmidt, A., and Stumpp, C.: Long-term data set analysis of stable
isotopic composition in German rivers, *Journal of Hydrology*, 552: 718-731,
http://dx.doi.org/10.1016/j.jhydrol.2017.07.022, 2017.

Rice, R., Bales, R. C., Painter, T. H., and Dozier, J.: Snow water equivalent along elevation
gradients in the Merced and Tuolumne River basins of the Sierra Nevada, *Water Resources
Research*, 47, W08515, doi: 10.1029/2010WR009278, 2011.

Rundel, P. W., Parsons, D. J., and Gordon, D. T.: Montane and subalpine vegetation of the Sierra
Nevada and Cascade Ranges, in: Barbour, M. G and Major, J. (Eds), *Terrestrial Vegetation
of California*, Wiley, New York, pp. 559-599, 1977.

Scalzitti, J., Strong, C., and Kochanski, A.: Climate change impact on the roles of temperature and
precipitation in western U.S. snowpack variability, *Geophysical Research Letters*, 43,
5361-5369, doi: 10.1002/2016GL068798, 2016.

Shaw, G. D., Conklin, M. H., Nimz, G. J., and Liu, F.: Ground water and surface water flow to the Merced River, Yosemite Valley, California: ^{36}Cl and Cl$^-$ evidence, *Water Resour. Res*., 1000   50,1943–1959, doi:10.1002/2013WR014222, 2014.

Sivapalan M., Takeuchi, K., Franks, S. W., Gupta, V. K., Karambiri, H., Lakshmi, V., Liang, X., McDonnell, J. J., Mendiondo, E. M., O'Connell, P. E., Oki, T., Pomeroy, J. W., Schertzer, D., Uhlenbrook, S., and Zehe, E.: IAHS Decade on Predictions in Ungauged Basins (PUB), 2003–2012: Shaping an exciting future for the hydrological sciences, *Hydrological* 1005   *Sciences Journal*, 48:6, 857-880, DOI: 10.1623/hysj.48.6.857.51421, 2003.

Sklash, M. G., Farvolden, R. N., and Fritz, P.: A conceptual model of watershed response to rainfall, developed through the use of oxygen-18 as a natural tracer, *Canadian Journal of Earth Sciences*, 13, 271-283, 1976.

Stewart, I. T., Cayan, D. R., and Dettinger, M. D.: Changes toward earlier streamflow timing across 1010   western North America, *Journal of Climate*, 18, 1136-1155, 2005.

Stewart, I. T: Changes in snowpack and snowmelt runoff for key mountain regions, *Hydrological Processes*, 23: 78-94, DOI: 10.1002/hyp.7128, 2009.

Taylor, S, Feng, X., Kirchner, J.W., Osterhuber, R., Klaue, B., and Renshaw, C. E.: Isotopic evolution of a seasonal snowpack and its melt, *Water Resources Research* 37(3), 759-769, 1015   2001.

Taylor, R. G., Scanlon, B., Döll, P., Rodell, M., van Beek, R., Wada, Y., Longuevergne, L., Leblanc, M., Famiglietti, J. S., Edmunds, M., Konikow, L., Green, T.   R.,   Chen,   J., Taniguchi, M., Bierkens, M. F. P., MacDonald, A., Fan, Y., Maxwell, R. M., Yechieli, Y., Gurdak, J. J., Allen, D. M., Shamsuddha, M., Hiscock, K., Yeh, P. J. F., Holman, I., and 1020   Treidel, H.: Groundwater and Climate Change, *Nature Climate Change*, 3, 322–329, doi:10.1038/nclimate1744, 2013.

Tennant, C. J., Crosby, B. T., and Sarah S. E.: Elevation-dependent responses of streamflow to climate warming, *Hydrological Processes*, 29, 991-1001, doi: 10.1002/hyp.10203, 2015.

Thompson, L. G., Mosley-Thompson, E., and Henderson, K.A.: Ice-core palaeoclimate records in 1025   tropical South America since the Last Glacial Maximum, *Journal of Quaternary Science*, 15, 377–394, 2000.

Vaughan, D. G., Comiso, J. C., Allison, I, Carrasco, J., Kaser, G., Kwok, R., Mote, P., Murray, T., Paul, F., Ren, J., Rignot, E., Solomina, O., Steffen K., and Zhang, T.: Observations:

Cryosphere. In: Climate Change 2013: The Physical Science Basis, Contribution of Working Group I to the Fifth Assessment Report of the Intergovernmental Panel on Climate Change, edited by: Stocker, T.F., Qin, D., Plattner, G.-K., Tignor, M., Allen, S. K., Boschung, J., Nauels, A., Xia, Y., Bex, V., and Midgley, P. M., Cambridge University Press, Cambridge, United Kingdom and New York, NY, USA, 2013.

Voss, K. A., Bookhagen, B., Sachse, D., and Chadwick, O. A.: Variation of deuterium excess in surface waters across a 5000-m elevation gradient in eastern Nepal, *Journal of Hydrology*, 586, https://doi.org/10.1016/j.jhydrol.2020.124802, 2020.

Wang, L., Caylor, K. K., and Dragoni, D.: On the calibration of continuous, high-precision δ^{18}O and δ^2H measurements using an off-axis integrated cavity output spectrometer, *Rapid Communications in Mass Spectrometry*, 23, 530-536, DOI: 10.1002/rcm.3905, 2009a.

Wang, N., Zhang, S., He, J., Pu, J., Wu, X., and Jiang, X.: Tracing the major source area of the mountainous runoff generation of the Heihe River in northwest China using stable isotope technique, *Chinese Science Bulletin*, 54: 2751-2757, doi: 10.1007/s11434-009-0505-8, 2009b.

Wen, R., Tian, L., Liu, F., and Qu, D.: Lake water isotope variation linked with in-lake water cycle of the alpine Bangong Co, arid western Tibetan Plateau. *Arctic, Antarctic and Alpine Research*, 48(3), 563-579, DOI: *http://dx.doi.org/10.1657/AAAR0015-028*, 2016.

Windhorst, D., Waltz, T., Timbe, E., Frede, H. G., and Breuer, L.: Impact of elevation and weather patterns on the isotopic composition of precipitation in a tropical montane rainforest, *Hydrol. Earth Syst. Sci.*, 17, 409–419, doi:10.5194/hess-17-409-2013, 2013.

Yanggen, D. A. and Born, S.: Protecting groundwater quality by managing local land use, *Journal of Soil and Water Conservation*, 45(2), 207-210, 1990.